

A Major-II Project Report

on

**Analysis of Cantilever Beam Using Digital Image
Correlation Technique Under Different Loading
Conditions**

submitted in partial fulfillment for the award of the degree

of

Master of Technology

in

**Mechanical Engineering
(Computational Design)**

by

Ajit Singh

(Roll No. 2K13/CDN/02)

under the guidance

Of

**Dr. R.C. Singh
(Assistant Professor)**

**Dr. Rajiv Chaudhary
(Assistant Professor)**



Department Of Mechanical Engineering

Delhi Technological University, Delhi

2014-15

DECLARATION

I hereby declare that the project work entitled “**Analysis of cantilever Beam Using Digital Image Correlation Technique under different loading conditions**” submitted to Delhi Technological University, is a record of an original work done by me under the guidance of Dr. Rajiv Chaudhary and Dr. R.C. Singh. This project is submitted in the partial fulfillment of the requirements for the award of degree of Master of Technology in Mechanical Engineering under specialization Computational Design. I further declare that the results embodied in this report have not been submitted to any other university or institute for the award of the diploma or degree.

Ajit Singh

Roll no. 2k13/CDN/02

CERTIFICATE

This is to certify that the project work entitled “**Analysis of Cantilever Beam Using Digital Image Correlation Technique Under Different Loading Conditions**” is being submitted by **Ajit Singh (2k13/CDN/02)** for the partial fulfillment for the award of **Master of Technology in Mechanical Engineering Under Specialization Computational Design** from the Delhi Technological University, Delhi-110042 during the academic session 2013-2015 is a authentic work carried out by him under our guidance and supervision.

The results embodied in this report have not been submitted to any other University or Institution for the award of degree or diploma and the declaration made by him is correct to the best knowledge and belief.

Dr. R.C. Singh
Assistant Professor
(Deptt. Of Mechanical Engineering)

Dr. Rajiv Chaudhary
Assistant Professor
(Deptt. Of Mechanical Engineering)

ACKNOWLEDGEMENTS

I take this opportunity to express my profound gratitude and deep regards to my supervisors **Dr. R.C. Singh** and **Dr. Rajiv Chaudhary** for their exemplary guidance, monitoring and constant encouragement throughout the course of this report. The blessing, help and guidance given by them time to time shall carry us a long way in the journey of life on which we are about to embark.

We take this opportunity to express a deep sense of gratitude to **Prof. R.S. Mishra (HOD Mechanical)**, and **faculty members** as well as **technical staff** for their cordial support, providing their valuable time, information and guidance, which helped me in completing this task through various stages.

I would also take this opportunity to thank my parents for their constant motivation and encouragement to strive towards my dream.

I would also like to thank my friends for their constant support through various stages which help me in completion of this project.

Ajit Singh

Roll. No. 2k13 /CDN/02

ABSTRACT

Most of the Materials fail due to strain ,in different loading conditions. Researchers are involved in the detection of the cause and propagation of the crack . Scientists are working on Digital image correlation (DIC) technique which is a non-contact strain measuring method. DIC provides the information regarding deformation in a specimen by processing two digital images that are captured before and after the deformation. Specimens (with and without hole) under different loading condition have been analyzed using DIC and the results have been assimilated with numerical techniques such as software package Solidworks. This study basically deals with the accuracy of measuring strain and crack tip deformation in the specimen. It has been found that type of loading and camera position affects the accuracy of the measurement of the strain and crack tip propagation. Further, It has been found that the crack propagates curving towards the location of the hole ,when the hole is present within a certain proximity from the line of the crack. Further it was concluded from the results that crack propagates in the same direction as indicated by the displacement fields and strain fields generated around crack tip, in DIC image, priors to its real time propagation.

List of Figures

| Figure No. | Topic | Page No. |
|------------|--|----------|
| 1.1 | Image showing test specimen undergoing tensile load | 6 |
| 1.2 | Results indicating strains and displacement at different points of specimen under tensile load | 7 |
| 1.3 | Outline of variable involved in DIC Technique | 9 |
| 1.4 | Portion of digital image showing height , width, rows and column | 10 |
| 3.1 | Setup containing various important component of DIC | 25 |
| 3.2 | Specimen 1 with hole as shown in figure | 26 |
| 3.3 | Specimen 1 (with crack without hole) | 27 |
| 3.4 | Specimen 2 without hole as shown in figure | 27 |
| 3.5 | Specimen 2 (with crack without hole) | 27 |
| 3.6 | Specimen grain under testing | 28 |
| 3.7 | Universal testing machine. | 31 |
| 3.8 | UTM loaded with specimen | 32 |
| 3.9 | Specimen2 after loading | 33 |
| 3.10 | Showing model of Specimen 1 on SOLIDWORKS | 34 |
| 3.11 | Showing model of Specimen 2 on SOLIDWORKS | 35 |
| 3.12 | Showing Specimen 1 under transverse loading condition | 35 |
| 3.13 | Showing Specimen 2 under transverse loading condition | 36 |

| | | |
|------|--|----|
| 3.14 | Showing Specimen1 under tensile loading condition | 36 |
| 3.15 | Showing Specimen 2 under tensile loading condition | 37 |
| 3.16 | Showing model of specimen 1 after meshing | 40 |
| 3.17 | Showing model of specimen 2 after meshing | 40 |
| 3.18 | Mess generated in ANSYS | 42 |
| 4.1 | Specimen 1 at F=545N | 45 |
| 4.2 | Specimen 1 at F=732N | 45 |
| 4.3 | Showing specimen 1 at load 395N and the crack | 46 |
| 4.4 | Showing Specimen 1 at load 410N and the condition of crack at this load | 46 |
| 4.5 | Shows the condition when crack propagates through hole | 47 |
| 4.6 | Specimen 2 under 455N | 48 |
| 4.7 | Showing processed image of the specimen2 at load 758N | 48 |
| 4.8 | Showing processed image of specimen 2 having straight load | 48 |
| 4.9 | Image showing v field in specimen 1 under the loading condition between 545N to 732N | 49 |
| 4.10 | Image showing the E field specimen1 under the load between 545N to 732N | 49 |
| 4.11 | Image showing v field n specimen 1 when the load 395N to 450N | 50 |
| 4.12 | Image showing e field in specimen 1 between the load 395N to 410N | 50 |
| 4.13 | Image showing v field in specimen 2(without hole) under load 545N to 758 N | 51 |
| 4.14 | Image showing distribution if e field in specimen 2 (without hole) under load 545 N to 758 N | 51 |

| | | |
|------|--|----|
| 4.15 | Showing Graph between Force and displacement in specimen 1 | 52 |
| 4.16 | Showing graph between load and displacement in specimen 2 | 52 |
| 4.17 | Showing tensile load applied on specimen 1 | 54 |
| 4.18 | Showing final state of the specimen when maximum loading ($F=760N$) has been done in specimen 1 | 55 |
| 4.19 | Showing zoomed image of final state of the specimen1 when maximum loading ($F=760N$) has been done in specimen | 55 |
| 4.20 | Showing displacement in the specimen 1 at different points | 56 |
| 4.21 | Showing stress(von mises) at different point in the specimen 1 | 57 |
| 4.22 | Showing crack tip area at the load of 760 N | 57 |
| 4.23 | Showing tensile load applied in specimen2 | 58 |
| 4.24 | Showing displacement produced in the specimen2 on tensile loading at load equals to 758N | 58 |
| 4.25 | Shows the von mises stress in specimen2 under tensile load of 758N | 59 |
| 4.26 | Shows the von mises stress in specimen2(near slit end) under tensile load of 758N | 60 |
| 4.27 | Showing Specimen 1 under transverse loading condition | 61 |
| 4.28 | showing von mises stress in specimen 1 under transverse loading. | 61 |
| 4.29 | showing displacement in specimen 1 under | 62 |

| | | |
|------|---|----|
| | transverse loading | |
| 4.30 | Showing Specimen 2 under transverse loading condition | 62 |
| 4.31 | Showing von mises stress in specimen 2 under transverse loading | 63 |
| 4.32 | Showing Specimen 2 under transverse loading condition | 63 |

List of Tables

| S.No. | Topic | Page No. |
|-------|--|----------|
| 3.1 | Showing specification of DIC camera | 25 |
| 3.2 | Showing properties of specimens used | 26 |
| 3.3 | Showing specification of UTM | 30 |
| 3.4 | Showing properties of specimen modeled in SOLIDWORKS | 38 |
| 3.5 | Showing property of specimen taken | 38 |
| 3.6 | Showing Detail of fixture kept | 39 |
| 3.7 | Showing detail of force(transverse) applied | 39 |
| 3.8 | Showing detail of force(tensile) applied | 39 |
| 3.9 | Showing meshing information | 41 |
| 3.10 | Showing meshing specification | 41 |
| 3.11 | Showing procedure and inputs to ANSYS | 44 |

CONTENTS

| | |
|---|-------|
| Declaration..... | (ii) |
| Certificate..... | (iii) |
| Acknowledgements..... | (iv) |
| Abstract..... | (v) |
| List of figures..... | (vi) |
| List of tables..... | (x) |
| | |
| Chapter 1 | |
| Introduction | 1 |
| 1.2 Digital Image Correlation Technique..... | 3 |
| 1.2.1 Method | 3 |
| 1.2.2 Uses..... | 4 |
| 1.2.3 Advantages..... | 5 |
| 1.3 Relating image resolution and specimen dimensions | 9 |
| 1.3.1 Relating Focal Length and Distance between Camera and Specimen..... | 12 |
| 1.4 Speckle Pattern..... | 12 |
| 1.5 Theory about Crack propagation and its modes :..... | 14 |
| Chapter 2 | |
| Literature Review | 17 |
| 2.1 Research gap | 23 |
| 2.2 Aim of the Study: | 23 |
| Chapter 3 | |
| Experimental Setup and Procedure | 24 |
| 3.1 DIC setup..... | 24 |
| 3.1.1 Digital camera..... | 24 |
| 3.2 Setup for crack growth propagation study : | 26 |
| 3.2.1 Specimen..... | 26 |
| 3.2.2 Load specification : | 29 |
| 3.3 Universal testing machine : | 30 |
| 3.3.1 Components: | 30 |

| | | |
|-----------|---|----|
| | 3.3.2 Specification of available UTM machine: | 31 |
| | 3.3.3 Uses of UTM..... | 31 |
| | 3.4 Experimental procedure of crack growth study on DIC : | 32 |
| | 3.4.1 Tensile loading :..... | 32 |
| | 3.4.2 Transverse loading:..... | 33 |
| | 3.5 Procedure of crack growth study on software packages (Numerical Techniques) | 34 |
| | 3.5.1 Transverse loading :..... | 35 |
| | 3.5.2 Tensile loading :..... | 37 |
| | 3.5.3 Material Properties..... | 38 |
| | 3.5.4 Fixture | 39 |
| | 3.5.5 Load | 39 |
| | 3.5.6 Meshing : | 40 |
| | 3.6 Analysis using ANSYS | 42 |
| Chapter 4 | Results and Discussions | 45 |
| | 4.1 Results of DIC analysis of crack tip propagation on Tensile loaded specimen: | 45 |
| | 4.2 Displacement field and strain field near crack tip :..... | 49 |
| | 4.3 Result of the UTM machine in crack tip propagation study of tensile loaded specimen | 52 |
| | 4.3.1 For specimen 1 :..... | 53 |
| | 4.3.2 For specimen 2:..... | 53 |
| | 4.4 Results obtained from solidworks:..... | 54 |
| | 4.4.1 Results for Specimen1 under tensile load :..... | 54 |
| | 4.4.2 Results for Specimen 2 under tensile load :..... | 58 |
| | 4.4.3 Transverse loading results in specimen 1: | 61 |
| | 4.4.4 Transverse loading results in specimen 2: | 62 |
| Chapter 5 | Conclusion and further scope of the study | 64 |
| | References | 65 |

INTRODUCTION

Strain measurements including crack growth and stress measurements are very important in mechanical sciences. A strain in any material can be defined as the coefficient of the change in length and the initial length. Strains are involved in many important material properties and parameters (i.e. Young's Modulus, Stress-Strain Curve, Poisson's Ratio, etc.). Strain measurements have been very important in development of the structural engineering theory. The capability to measure strain precisely & accurately will become increasingly more important for field monitoring for products that had been made during the boom of infrastructure in the last century continue to deteriorate with age. Engineers thus required detailed strain data taken in a various locations on the complex structures so that they can accurately and precisely find their remaining service life and capacity. Most of the Materials fails due to strain in different loading conditions. Researchers are involved in the detection of the cause and propagation of the crack. Recently, on strain measurements at any point inside an area of interest, complex investigations has been done to enrich the study of the behavior of materials and structural components. That is why, researchers are very much interested on a strain map over an entire surface of the specimen. Some passé instruments, used to measure strains (i.e. strain gauge and LVDT etc) are not that much accessible and equipped to draw strain maps, because it would be very uneconomic and not that much practical. Now according to this fact that strain maps have been required to perform new function, a nascent technology has been developed so that these desired results can be obtained. It has been done similarly in the case of crack growth measurements, and in strain analysis.

The two most widely and commonly used methods for calculating displacement have several significant disadvantages, these methods includes vibrating wire and foil strain gauges. They are only capable of giving linear point readings of strain, which implies a significant number of gauges have been required in order to measure strain distribution or fields. Also, each one of these

gauges has to be placed separately, and so the final number of gauges are often limited by wiring and data acquisition constraints. Moreover Foil gauges have long-term stability issues and so, and thus they can be used in the laboratory, they are not generally appropriate for long-term field monitoring which is the need of today's world. Vibrating wire strain gauges are much more stable but the cost of each gauge makes them quite expensive for the type of pervasive monitoring that would be required to validate complex structural projects. Finally, both foil and vibrating wire gauges need to be stick to the structure, which can have a significant impact on the strain measurements if the stiffness of the structural material is not significantly greater than the stiffness of the strain gauge, this certainly adds another limitation.

Knowing to this fact that strain maps have been required to perform new functions, a nascent technology has been developed so that these desired results can be obtained. This technology is the Digital Image Correlation (DIC) technique, which gives a contour map of strains of an entire specimen surface undergoes mechanical tests. Scientists are working on Digital image correlation (DIC) technique applied for a whole field and non contact strain measuring method DIC represents an alternative to conventional strain gages for measuring surface strains in that it overcomes many of the disadvantages outlined above. DIC compares two digital images (one reference image and a deformed image) in order to determine how much movement or we can say deformation has occurred amidst the two. This movement or displacement thus can then be used to determine strains, crack growth, stresses. It should be noted that since the technique requires the use of digital cameras, it is not suitable for measuring internal strains or strains in products that are not visually accessible. For the monitoring of existing structures, these accessibility limitations also apply to conventional strain gauges as well, and so this technique could be a potential replacement of conventional techniques. Until now DIC has been used as an alternative strain measurement technique in controlled lab settings but has shown promise for field monitoring. However, in order to attempt to use this technique for field monitoring, improved strain measurement accuracy is required . Other issues that are field specific, such as varying light conditions and temperature changes, still need to be addressed in greater detail, and are the subject of ongoing research. DIC is a noncontact deformation measuring method. It could provide information of deformation of a specimen by processing two digital images that are captured before and after the deformation. If we compared it to the requirements of the traditional optical measurements, such as holography, photoelasticity, and interferometry DIC is a simple , easy and economic method because it takes advantage of the natural speckle pattern on the specimen surface and only digital images taken by charge coupled device (CCD) camera are processed.

The following project examines the results of a series of tests conducted on a specimen plate in tension to determine what level of strain resolution can practically be achieved and how crack travel under the loading condition. The test setup will be introduced and the strain measurements and deformation from the first test will be discussed , Those results shows that the out-of-plane movement of the test specimen has a significant impact on the strain measurements.

1.1 Digital Image Correlation Technique

Digital Image Correlation (DIC) is a technique which is a noncontact in nature for measuring strain and displacement. It is quite simple to use in practical applications and economic as assimilate to other techniques such as interferometry and other conventional techniques. It is more accurate and subjective than manual measurement methods, leading to a myriad range of critical applications. Researchers are involved and indulged in enhancing the technique to enable its use for measurements involved during functioning of the product or machine even outside the laboratory. It is enhancing systems to apply DIC to the standardizing of materials ,machine and products and the supervising of engineering equipment, as well as execution in the civil as well as nuclear industries. It is also enlarging its use into very competitive environment , such as enhancing DIC so that it can be used over a laps of time without a need for a permanent set up , and using it to difficult to reach areas via small unmanned objects packed with camera and GPS instruments.

1.1.1 METHOD

DIC works by comparing digital photographs or images of a specimen at various stages of deformation. By detecting pixels, the system can determine surface displacement and can form 2D fields and 3D fields of deformation vector and strain maps. For DIC to work effectively, the pixel blocks requires to be unique and random following a range of contrast as well as intensity levels. It also requires no special sharpening and in most of the cases the real surface of the specimen's structure or component has enough image texture for Digital image correlation to work without the requirement for any specific surface preparation. Software techniques have been enhanced to obtain sub pixel resolutions and allow effective function of the algorithms. These changes allow a very high resolution measurements to be done such that with the help of commercially available cameras, surface deformation can be measured as to a part per million of view field . Images or photograph can be taken from a myriad variety of sources which includes conventional CCD or digital cameras, fast-speed videos, and microscopes, involving electron and atomic microscopes.

The correlation process in the DIC is not constrained to optical images only it can also be used on other data sets such as for finding roughness of surface , 2 dimensional surfaces of structures.

1.1.2 USES

DIC is not so complex to implement, it gives cost effective and trustworthy results which in a way lead it such that it can be used in variety of applications. It has been used to determine and calculating the strain in diverse range of application ,materials, specimen also included in detection of damage crack tip propagation deflection in surfaces, mapping of high strains, damages in materials such as composites , and vibration analysis in the systems. Researchers has implemented this techniques in wide range of problems and got to know that it is fit for the measurement of residual stress in practical applications such as hole drilling in small structures. Other projects have used the DIC for thermal expansion measurements and electronic components distortion detection, more over mechanical properties of nuclear materials have been measured using this technique .

Detection of damage in silk print screens and three dimensional shape measurement of air bags, strain development evolved during the processing of chocolate in chocolate manufacturing industries. Researchers are nowadays being involved in as a part of IMPACT (Innovative Materials, Monitoring, Design of Power Plants to Accommodate Carbon Capture), a major project that aims on reduction of carbon emission in the form of carbon dioxide from the carbon emitting industries which most of the time used to neglect this issue. The aim is to develop in-process monitoring of components of power plant to enhance service life and also helps in minimizing emissions. Researchers are using this technique (DIC) to standardized the new steels being enhanced in the project so that it can improve the high temperature capability of thick welded section of high alloy steel equipments. Which in a way leads to advancement techniques involved in-service monitoring which in terns enable plant to operate maximum temperatures under challenging environments.

Researchers are working to evolve promote the use of this technique through participation in relevant projects as well as through consultancy services for measurement to industry. The current focus of the researchers in DIC work is to give a practical technique that can be used in a wide range of applications, which includes monitoring strains in rail and bridges on roads and for determining crack opening in civil components precisely in the nuclear industry and power plants. Initial feasibility studies has shown that this technique has great potential in these areas.

1.1.3 ADVANTAGES

DIC has several advantages over conventional NDT methods and some of the other techniques includes optical as well, which are normally more uneconomic and more difficult to use in practical condition outside the lab because they require precise setup and very low vibrational conditions, This technique uses conventional digital images and in addition with surveying techniques also used in civil engineering, can be used to give quit accurate results of structures in practical environment. Any changes in the components or specimen or structure, easily be assimilate to the captured images and so external factors or we can say environmental factors that might cause unexpected changes ,can be detected, like any creature landing on a bridge can be easily detected. For the large buildings , and structures and power generation structure, manual inspection techniques are still often used. This may leads to the errors that can enters into calculations as it includes human activity .And also it will then depend on the skill of the operator , But by taking exactly positioned and precise and accurate images , assimilation can be made between surveys and the differences can be readily identified, whether these are due to crack opening ,change in surface or deformation. The property that this technique is very cost effective and economic and also easily apply in practical forces researchers to take this technique in future endeavors. In this technique the main challenge for subsequent measurements is to give suitable ways of adjusting the camera. One example indicating the use of this technique is in measurement of crack opening. Say a specimen made of concrete that is reinforced as well, undergoing test that includes a load, then it would be very easy to determine the location and position of the main crack. But other minor cracks can also be present which cannot be detected manually .but using special paint or die can help in the identification of minor crack, By using this DIC technique, as images are taken before and after the crack opening thus crack opening study can easily be done. This further has the upper hand of detecting cracks that have opened, in economic and non contact way. Even the edges of the crack are badly defined ,this technique can also give exact and precise measurement of crack opening, and can provide useful information on where to apply sensors used for crack opening. In spite of the advantages this technique still have significant challenges in front of it, these includes the environmental ,weather , corrosion , droplets on camera lens that can constraint the use of this technique in practical outdoor activities. Thus the researchers are working on this to rectify these types of problems, working on exact repositioning of camera. Recently researchers also involved in enhancing new software and partnering with the firms

with the promise of use of DIC and develop new levels of accuracy, having aim in mind that this technique will become prominent in the world in the field of the strain detection.

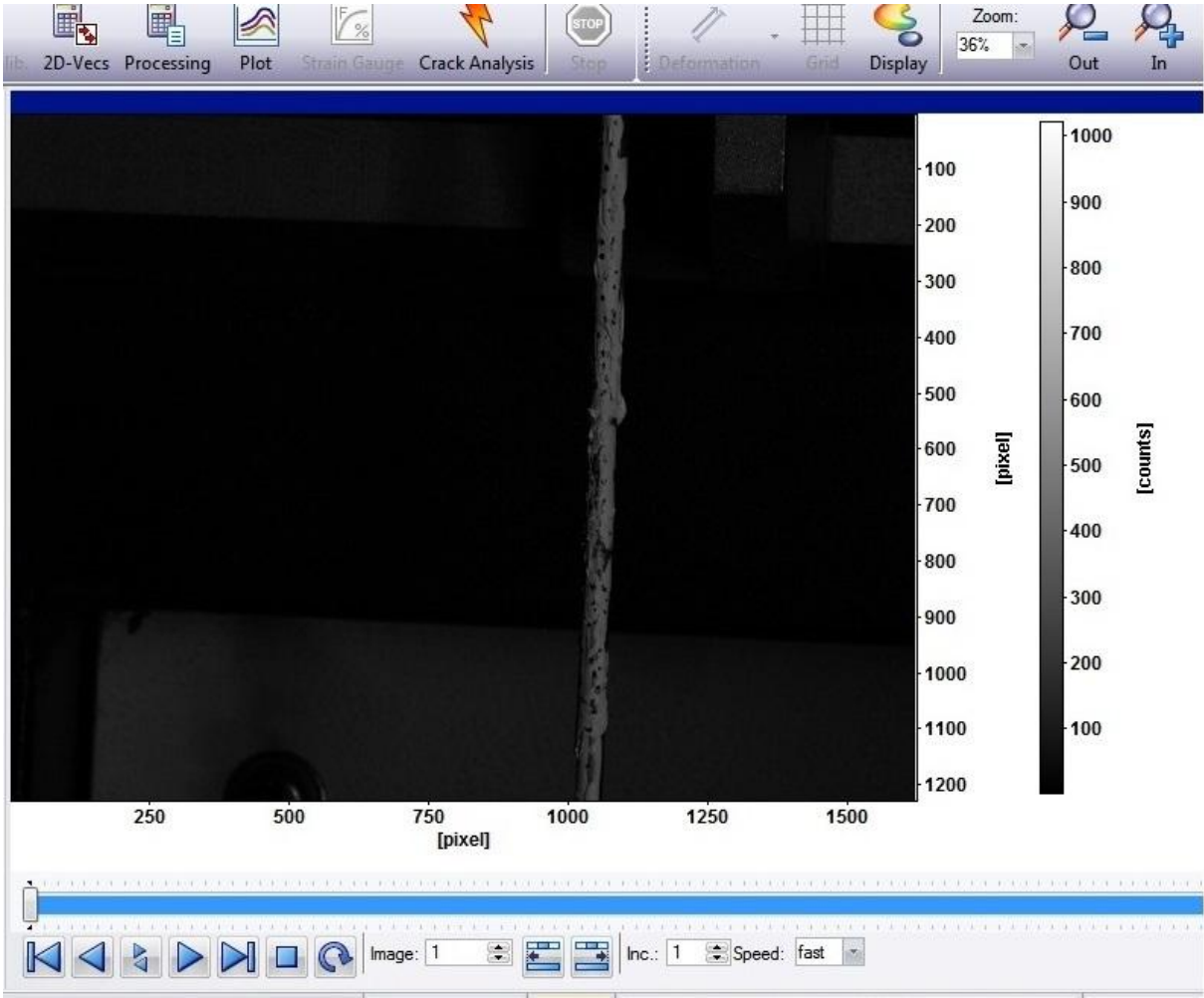


Figure 1.1 Image showing test specimen undergoing tensile load

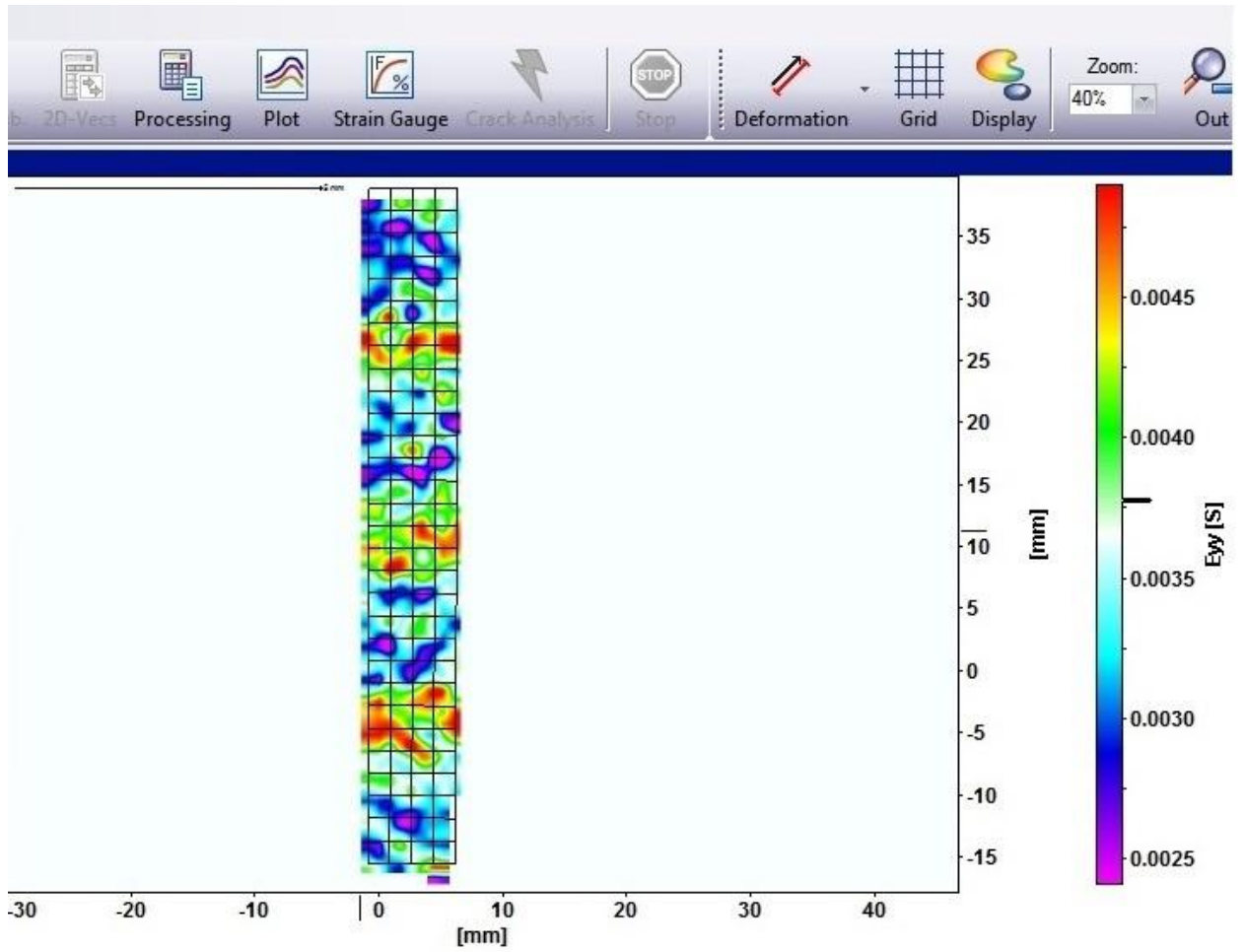


Figure 1.2 Results indicating strains and displacement at different points of specimen under tensile load

Figure 1.1 and 1.2 shows the experimental images taken by DIC camera and results in the form of graph for strain and displacement at various points is shown.

The digital image correlation works on correlation analysis ,mathematical in nature, to get digital image data taken while the specimens are under mechanical tests. This technique is based on capturing the images continuously with a dg camera during the period of deformation to examine the change in surface properties and the behavior of the specimen is understood when increasing loads are applied on it. To use this method, the specimen needs to be prepared on the surface , which is done by dotted pattern also known as speckle pattern .

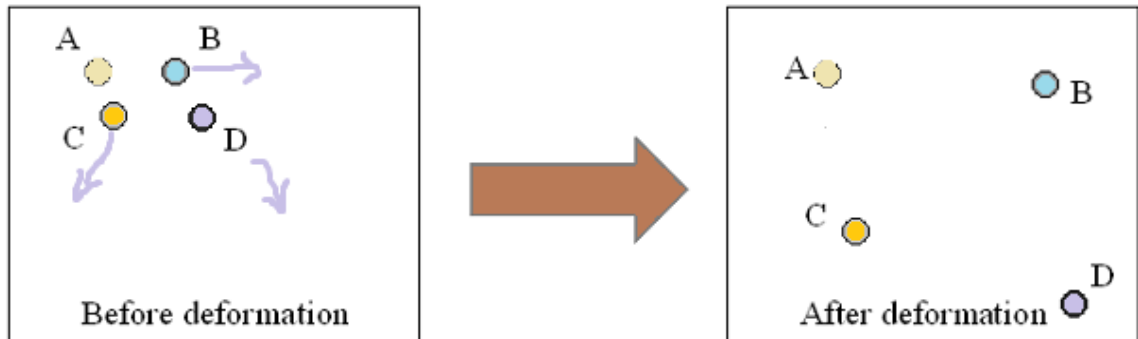
On using the discrete pixels of a digital image and their grey level values for intensity, these data are recorded as a two-dimensional array. Under the assumption that there is a one-to-one correspondence on the intensity pattern of two images taken before and after a deformation increment, one could deduce the information of deformation from the intensity pattern. To remain within the limit of linear approximation of the deformation, a region of pixels called subset should be small enough. If a subset is arbitrarily chosen from the image taken before a deformation

increment and a reference point (x_0, y_0) as well as a nearby point (x, y) is selected from this subset, the position (x', y') of the nearby point after the deformation increment could be described as

$$x' - x = u + \frac{\partial u}{\partial x} dx + \frac{\partial u}{\partial y} dy,$$

$$y' - y = v + \frac{\partial v}{\partial x} dx + \frac{\partial v}{\partial y} dy,$$

where (u, v) are the displacements of the reference point, and (dx, dy) are the position differences of the reference point and the nearby point before deformation. The components of the first-order displacement gradient are. Since only a two-dimensional deformation is considered in the above equations, one needs two displacement components and four displacement gradient components to describe the position of a nearby point. This digital image correlation technique starts with image known as base image, then a continuous myriads of images are taken during the process known as deformed image. All the distorted images show a different pattern of dots relative to the base image. With the help of software these differences between dotted patterns can be evaluated by correlating all the dots of the base image and any distorted image, and a strain map can be created.



This image shows four dots of different shapes thus represent the different pixels. The image after deformation shows the same four dots, but now represents other four pixels. The software measures the difference between dots location (pixels) of the different images and correlates them to determine the deformation.

The digital image correlation requires computer software and a good digital camera. For getting precise images using DIC technique it is very crucial to consider some variables. The results are very much related to the resolution of digital camera (pixels columns \times pixels rows), the width (b) and the height (a) of the specimen, focal length of the lens (F), the distance between camera and specimen (d), and the application of the speckle pattern.

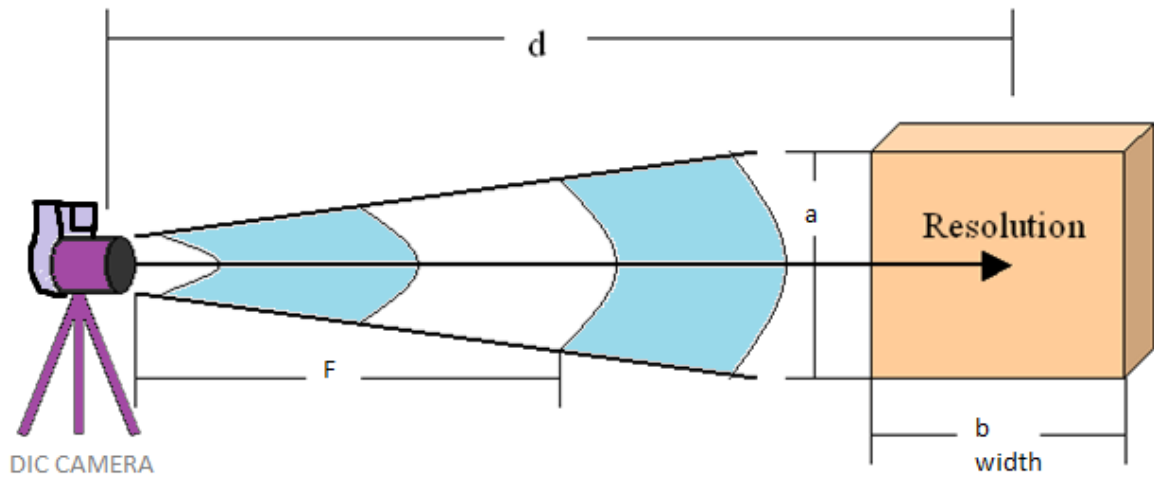


figure 1.3 Outline of variable involved in DIC Technique

1.2 RELATING IMAGE RESOLUTION AND SPECIMEN DIMENSIONS

The resolution is the indicator of pixels in an image and if more resolution that means more detail we can take from that image. A relation can be established between the specimen surface are and the image and we can get to know about the area that the particular pixel going to occupy in the surface. To find how much space has been represented by a pixel in an image of the specimen, the dimensions of the specimen (height and width) need to be divided by the camera resolution (pixel rows and pixel columns). Following equation can be used to indicate above said.

$$\zeta_w = \frac{b}{r} \quad \text{(equation 1)}$$

$$\zeta_h = \frac{a}{c} \quad \text{(equation 2)}$$

With the help of the first equation the calculation related to the width of the pixel represented on the image of the specimen can be done, where ζ_w is the width of the pixel, c represents the pixel

columns numbers, w is used to represent the width of the specimen. With the help of the second equation the calculation related the height of the pixel can be done, where ζh is used to indicate the height of the pixel, a is used to indicate the height of the specimen and r is used to represent pixel rows numbers. With increase in the resolution, the ζ value will decrease, and as the dimensions of the specimen increases, the ζ value will increase., the values represented by ζb and ζa for particular specimen always are equal Independent of the dimensions of the specimen.

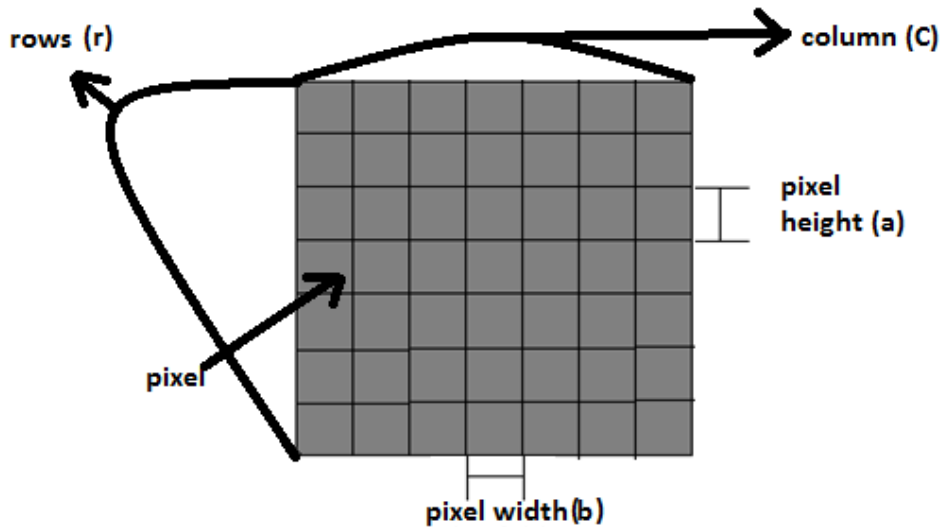


Figure1.4 Portion of digital image showing height ,width, rows and column

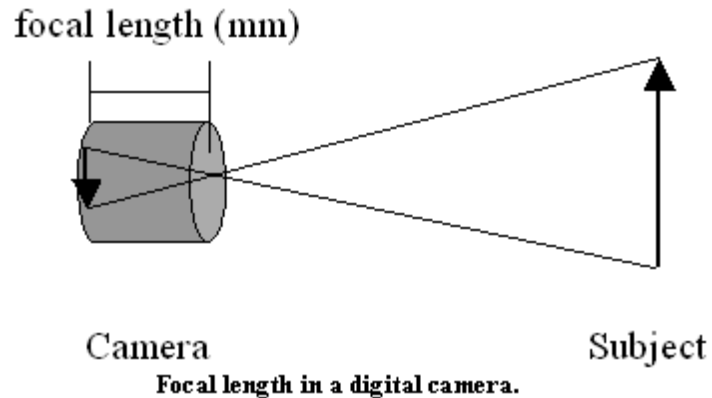
A 4:3 or a 3:2 aspect ratio is common in most of the resolutions of the digital camera. The most common digital cameras have an aspect ratio of 4:3 which in terms of resolution of image can be 1024×768 , 800×600 etc .4:3 Aspect ratio is going to be used for the understanding of relation between resolution of image an dimensions of the specimen . in order to maximize the area of pixels used it become important that the samples must occupy the ,maximum space as large as possible in an image . 4:3 aspect ratio become helpful for the ideal surface area related to the specimens that it can use maximum pixels in an image. This comes out to be is a rectangle with a 4:3 aspect ratio we can say like $4. \times 3.$, $12. \times 9.$, etc. In this case, both first and second equations can be used.

There are some constraints in using the first equation if the area of the surface of the specimen is a rectangle a square or, and having its wide is less than 1.33 times that of its height, then only second equation can be considered ,the first equation cannot be entertained, the reason being that all the pixel columns are not going to be used to indicate the specimen in the image. It is the

known fact that if the specimen is square the number of pixel columns that are going to indicate the specimen in the image are going to be in equal numbers as that of pixel rows, but not in case of the specimen which is rectangle. In case of the specimen of rectangular surface this can be done with the help of geometry, but not necessarily, as the results of both the equations always going to be the same. So just row of the pixel and height of the specimen is to be needed.

1.2.1 Relating Focal Length and Distance between Camera and Specimen

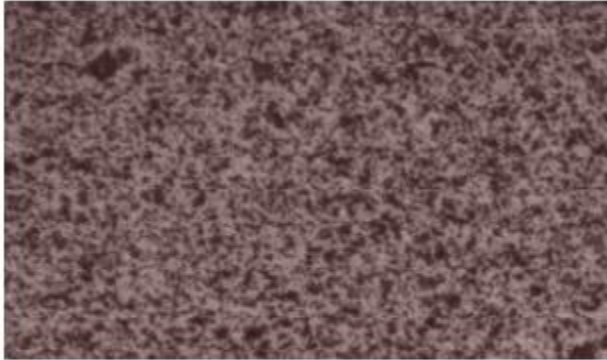
The focal length is the distance in millimeters between the optical center of the lens and the focal point in the surface of the sensor of the camera when the subject is in focus (See Figure). There are three categories for the focal length. The three categories are wide angle lens (focal length < 35 mm), normal lens ($35 \text{ mm} < \text{focal length} < 55 \text{ mm}$) and telephoto lens (focal length $> 55 \text{ mm}$). The higher the focal length, the closer the image is going to be registered in the digital camera.



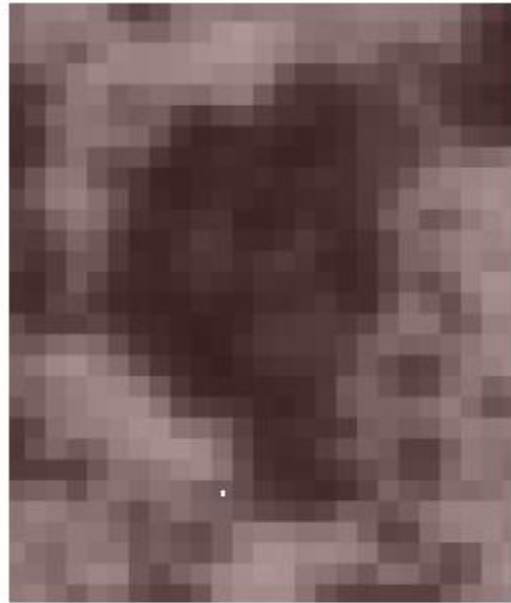
It is not necessary to know an exact distance or focal length for each different specimen dimensions, because they can be adjusted in different ways to get the specimen focused with the camera. If the camera needs to be very far from the specimen, the image can be focused by using a long focal length and vice versa. The distance between camera and specimen also depends on the specimen dimensions. The higher the specimen dimensions, the higher the distance between camera and specimen will be needed.

1.3 Speckle Pattern

The specimen surface to be studied must have a random dot pattern. The speckle pattern is essential, because it permits the software to be able to identify and calculate the displacements with accuracy. To obtain accurate results with the digital image correlation it is important to get an adequate speckle pattern. An adequate speckle pattern must have a considerable quantity of black speckles with different shapes and sizes (See Figure). The effectiveness of the speckle pattern can be determined by the quantity of pixels per black speckle. A good speckle pattern must have small black speckles (10 pixels), medium black speckles (20 pixels) and large black speckles (30 pixels). The quantity of pixels per black speckle size is approximated (See Figure)



A good speckle pattern



**A medium black speckle zoomed.
The black speckle has approximately 15 pixels
wide and 20 pixels high.**

To identify the ideal size of any black speckle in a specimen, a relation between the black speckle size desired (small, medium or large) and the quantity of space represented by a pixel in a specimen image (ζ_b or ζ_a) can be made. Knowing the quantity of pixels that any black speckle size must have and the pixel size represented in a specimen image, their product are going to give us the proper dimensions of the black speckles in the specimen.

The equation 3 allows to calculate the dimensions of a black speckle in a specimen, where ζ is the black speckle length in a specimen, p is the quantity of pixels that the desired black speckle size must have and ζ is the pixel size represented in a specimen image (ζ_b or ζ_a) (See Figure). It is important to notice that the results of ζ are an approximation to have an idea of how the black speckles length must be in any specimen. Also, to get accurate results is very important to avoid black speckles bigger than the large black speckles.

1.4 Theory about Crack propagation and its modes :

Stress and displacement fields around a crack tip of a linear elastic isotropic material are written separately for all the three modes:

1. Mode I,

2. Mode II,

3. Mode III.

It is to be noted that the Greek letter μ has been used to denote the shear modulus, usually written as G, so that it should not be confused for the strain release rate, $\dot{\epsilon}$. Also, the small differences among the formulas for plane stress cases and plane strain cases are handled by κ , where

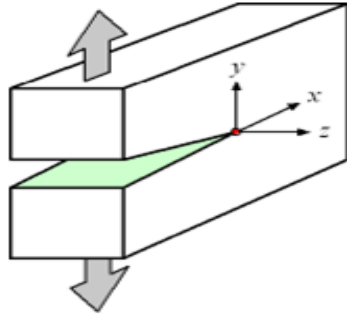
$$\kappa = \begin{cases} \frac{3-\nu}{1+\nu} & \text{(Plane Stress)} \\ 3-4\nu & \text{(Plane Strain)} \end{cases}$$

For linear elastic materials, the principle of superposition applies. A mixed-mode problem can be treated as the summation of each mode.

Bellow equations are taken from Andresen's Fracture mechanics .

$$\sigma_{ij}^{(Total)} = \sigma_{ij}^{(I)} + \sigma_{ij}^{(II)} + \sigma_{ij}^{(III)}$$

Mode I :



$$\sigma_{xx} = \frac{K_I}{\sqrt{2\pi r}} \cos\left(\frac{\theta}{2}\right) \left[1 - \sin\left(\frac{\theta}{2}\right) \sin\left(\frac{3\theta}{2}\right)\right]$$

$$\sigma_{yy} = \frac{K_I}{\sqrt{2\pi r}} \cos\left(\frac{\theta}{2}\right) \left[1 + \sin\left(\frac{\theta}{2}\right) \sin\left(\frac{3\theta}{2}\right)\right]$$

$$\sigma_{zz} = \begin{cases} 0 & \text{(Plane Stress)} \\ \nu(\sigma_{xx} + \sigma_{yy}) & \text{(Plane Strain)} \end{cases}$$

$$\tau_{xy} = \frac{K_I}{\sqrt{2\pi r}} \cos\left(\frac{\theta}{2}\right) \sin\left(\frac{\theta}{2}\right) \cos\left(\frac{3\theta}{2}\right)$$

$$\tau_{yz} = 0$$

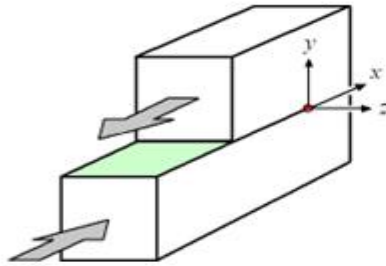
$$\tau_{zx} = 0$$

$$u_x = \frac{K_I}{2\mu} \sqrt{\frac{r}{2\pi}} \cos\left(\frac{\theta}{2}\right) \left[\kappa - 1 + 2\sin^2\left(\frac{\theta}{2}\right)\right]$$

$$u_y = \frac{K_I}{2\mu} \sqrt{\frac{r}{2\pi}} \sin\left(\frac{\theta}{2}\right) \left[\kappa + 1 - 2\cos^2\left(\frac{\theta}{2}\right)\right]$$

$$u_z = 0$$

Mode II



$$\sigma_{xx} = -\frac{K_{II}}{\sqrt{2\pi r}} \sin\left(\frac{\theta}{2}\right) \left[2 + \cos\left(\frac{\theta}{2}\right) \cos\left(\frac{3\theta}{2}\right)\right]$$

$$\sigma_{yy} = \frac{K_{II}}{\sqrt{2\pi r}} \sin\left(\frac{\theta}{2}\right) \cos\left(\frac{\theta}{2}\right) \cos\left(\frac{3\theta}{2}\right)$$

$$\sigma_{zz} = \begin{cases} 0 & \text{(Plane Stress)} \\ \nu(\sigma_{xx} + \sigma_{yy}) & \text{(Plane Strain)} \end{cases}$$

$$\sigma_{xy} = \frac{K_{II}}{\sqrt{2\pi r}} \cos\left(\frac{\theta}{2}\right) \left[1 - \sin\left(\frac{\theta}{2}\right) \sin\left(\frac{3\theta}{2}\right)\right]$$

$$\tau_{yz} = 0$$

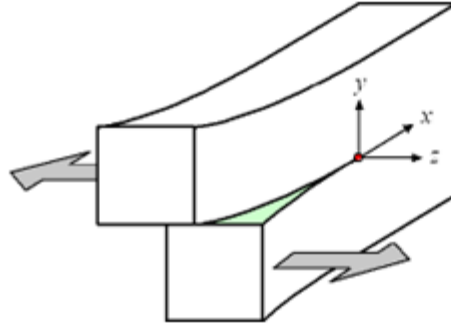
$$\tau_{zx} = 0$$

$$u_x = \frac{K_{II}}{2\mu} \sqrt{\frac{r}{2\pi}} \sin\left(\frac{\theta}{2}\right) \left[\kappa + 1 + 2\cos^2\left(\frac{\theta}{2}\right)\right]$$

$$u_y = -\frac{K_{II}}{2\mu} \sqrt{\frac{r}{2\pi}} \cos\left(\frac{\theta}{2}\right) \left[\kappa - 1 - 2\sin^2\left(\frac{\theta}{2}\right)\right]$$

$$u_z = 0$$

Mode III



$$\sigma_{xx} = 0$$

$$\sigma_{yy} = 0$$

$$\sigma_{zz} = 0$$

$$\tau_{xy} = 0$$

$$\tau_{yz} = \frac{K_{III}}{\sqrt{2\pi r}} \cos\left(\frac{\theta}{2}\right)$$

$$\tau_{zx} = -\frac{K_{III}}{\sqrt{2\pi r}} \sin\left(\frac{\theta}{2}\right)$$

$$u_x = 0$$

$$u_y = 0$$

$$u_z = \frac{K_{III}}{\mu} \sqrt{\frac{r}{2\pi}} \sin\left(\frac{\theta}{2}\right)$$

□

Where KI, KII and KIII are the stress intensity factor for mode I, mode II and mode III respectively.

LITERATURE REVIEW

Peters and Ranson [1] employed DIC for displacement and strain measurement under the assumption that there is a one-to-one correspondence on the intensity pattern of surface images before and after deformation. Two displacements and four displacement gradients were searched for in-plane deformation. To achieve better accuracy on the deformation components, Sutton [6] discussed the effects of some key parameters and recommended that it was better to use nonlinear interpolation, 12-bit quantization, and high frequency sampling. Plastic incompressibility and thin-sheet assumptions was used by Wattrisse et al. [7] to derive the third displacement component, and Lu and Cary [8] refined DIC by implementing a second order approximation of the displacement gradients. A compensation algorithm was introduced for improving the correlation coefficient and increasing measuring accuracy by Jin et al. [9] and then a wavelet de-noise processing was adopted. Recently, an improved method based on the iteration and spatial-gradient was developed, and both finite element method and two-dimensional generalized cross-validation algorithm were adopted for smoothing the displacement field [10]. Luo et al. [11] utilized a pinhole camera model to express the transformation relating three dimensional world coordinates to two-dimensional computer-image coordinates by means of camera extrinsic and intrinsic parameters. In addition, DIC has been applied to the measurement of surface profile [12], the heterogeneous deformation of polymeric foams [13], the full-field deformation monitoring of fiber composite pressure vessel [14], and high strain gradient measurements [15]. MohammadrezaYadegari Dehnav et.al [16] studied Utilizing digital image correlation to determine stress intensity factors and the digital image correlation (DIC) technique was employed to evaluate the in-plane stress intensity factors (SIFs), KI and KII, for the contact between a half plane with an edge crack and an asymmetric tilted wedge. DIC requires two digital images of the same sample at different stages of loading to measure the corresponding displacements and strain fields. DIC method was utilized to evaluate SIFs in the contact problem between a half plane with an edge crack and an asymmetric tilted wedge. The effect of wedge tip angles on SIF values was studied for two different crack angles (60 and 90) under three different force magnitudes. The results of DIC method were compared with the ones obtained from the photoelasticity technique and revealed that the relative difference

between the SIF values obtained from the two methods was less than 3% for all the studied cases. This relative difference increased as a larger vertical force was applied on the specimens. DIC method could be a reliable alternative for the classical photoelasticity technique where the magnitude of the applied force. Y.G. Wangan et al. [17] studied a high resolution DIC technique for measuring small thermal expansion of film specimens and found that by using a reference glass–ceramic material of very low thermal expansion, a high-speed digital camera, and some improvements in the experimental set-up and post digital image processing, a high resolution digital image correlation technique for smaller thermal strain measurements was established. The CTE measurements on a thin Invar-like material and a thin poly-silicon plate were performed by this technique. The results were found to be 1.24 ppm/1C and 2.69 ppm/1C, respectively. Jay D. Carroll et al. [18] focused on High resolution digital image correlation measurements of strain accumulation in fatigue crack growth and found that Microstructure plays a key role in fatigue crack initiation and growth. Consequently, measurements of strain at the micro structural level are crucial to understanding fatigue crack behavior. The few studies that provide such measurements have relatively limited resolution or areas of observation. In this paper quantitative, full-field measurements of plastic strain near a growing fatigue crack in HastelloyX, a nickel-based super alloy was done. Unprecedented spatial resolution for the area covered was obtained through a novel experimental technique based on digital image correlation (DIC). These high resolution strain measurements were linked to electron backscatter diffraction (EBSD) measurements of grain structure(both grain shape and orientation). Po-Chih Hung.et al. [19] studied In-plane strain measurement by digital image Correlation and presented a "fast and simple" (FAS) detection algorithm based on the digital image correlation for measurement of the surface deformation of planar objects. The proposed algorithm uses only fine search at the pixel level resolution and surface fitting for sub-pixel level. Two different specimens are investigated to explore the feasibility of this proposed algorithm. The displacements calculated by the FAS algorithm are compared with the ones obtained from Newton-Raphson method (N-R) and Enhanced Sequential Similarity Detection Algorithm (ESSDA). The results show that the experimental data are in good agreement with the theoretical solution. The proposed algorithm is found to be much faster than Newton-Raphson method with inferior, yet reasonable, accuracy for displacement and strain evaluation in the cases of uniaxial tension and disk under diametrical compression tests. S.Tamulevicius, et al. [20] focused on thermal strain measurements in graphite using electronic speckle pattern interferometry and proposed has been and successfully tested to control this parameter using the real samples of graphite from ignalina npp units. C.J. Tay et al. [21] studied

Digital image correlation for whole field out-of-plane displacement measurement using a single camera and developed a simple method for whole field out-of-plane displacement measurement using only one camera. The proposed method employs digital image correlation to calculate an apparent in-plane displacement field which is introduced by magnification change due to an unknown out-of-plane displacement. To testify the possibility of the proposed method for measurement of non-structured object, a plate with a step of height 1.4 mm on its surface is used. Images of the step before and after an out-of-plane displacement are captured and the proposed method is used to determine the unknown out-of-plane displacement. Xiang Guo. et al. [22] studied Digital image correlation for large deformation applied in Ti alloy compression and tension test and found that digital speckle correlation is used in the measurement of Ti alloy compression and tension test. The key technologies applied in the measurement were discussed in detail, including camera calibration with telephoto lens and digital image correlation in large deformation. Single camera self-calibration algorithm based on photogrammetry were proposed. A large deformation measurement scheme, updating reference image scheme, was proposed. Shun-Fa Hwang et al. [23] focused on Strain measurement of SU-8 photo resist by a digital image correlation method with a hybrid genetic algorithm and found that the grip displacement of the MTS micro force testing system should not be used to calculate the strain because of the possible extension from the end sections. The strains obtained by DIC with single region are reasonable, but there are some variations from the method itself and from the different points selected on the specimen. These problems could be smeared out if double region is used in digital image correlation, and the strains obtained are accurate. Hence, it should be recommended. M.A. Sutton .et al. [24] studied The effect of out-of-plane motion on 2D and 3D digital image correlation measurements and confirmed that the theoretical equations are in excellent agreement with experimental measurements. Specifically, results show that (a) a single-camera, 2D imaging system is sensitive to out-of-plane motion, with in-plane strain errors (a-1) due to out-of-plane translation being proportional to DZ/Z , where Z was the distance from the object to the pin hole and DZ the out-of-plane translation displacement, and (a-2) due to out-of-plane rotation were shown to be a function of both rotation angle and the image distance Z ; (b) the telecentric lens has an effective object distance, Z_{eff} , that was 50 mm larger than the 55mm standard lens, with a corresponding reduction in strain errors from 1250 $\mu\text{m}/\text{mm}$ of outof- plane motion to 25 $\mu\text{m}/\text{mm}$; and (c) a stereovision system measures all components of displacement without introducing measurable, full-field, strain errors, even though an object may undergo appreciable out-of-plane translation and rotation. Zhengzong Tanga,et al. [25] studied Large deformation measurement

scheme for 3D digital image correlation method and found that Using this method, not only extremely large deformation can be measured successfully but also the accumulated error could be controlled. A polymer material tensile test and a foam compression test are used to verify the proposed scheme. Experimental results show that up to 450% tensile deformation and 83% compression deformation can be measured successfully. Rui Zhang,et al. [26] focused on Measurement of mixed-mode stress intensity factors using digital image correlation method in which the effect of the rigid body motion on the measured displacements was studied , then eliminated using the computed rigid body translation and rotation. A coarse-fine searching method was developed to determine the crack tip location. For validation, the SIF thus determined is compared with theoretical results, confirming the effectiveness and accuracy of the proposed technique. Therefore it reveals that the DIC is a practical and effective tool for full-field deformation and SIF measurement. It is found that the measured SIF is in good accordance with theoretical data, conforming the effectiveness and accuracy of the present technique. Mohammad Kashfuddoja et al. [27] focused on the Study on experimental characterization of carbon fiber reinforced polymer panel using digital image correlation. In which the properties are evaluated based on full field data obtained from DIC measurements by performing a series of tests as per ASTM standards. The evaluated properties were compared with the results obtained from conventional testing and analytical models and they were found to closely match. It was found that the subset size had more influence on material properties as compared to step size and their predicted optimum value for the case of both matrix and composite material was found consistent with each other. The aspect ratio of region of interest (ROI) chosen for correlation should be the same as that of camera resolution aspect ratio for better correlation. Xiangjun Dai et al. [28] studied Strain field estimation based on digital image correlation and radial basis function. In which Two methods based on digital image correlation (DIC) and radial basis function (RBF) were proposed to obtain the accurate strain field in this paper. One was a combined method. RBF was applied to remove the noisy discrete displacement data first. After that, the strain was computed by a local least-squares algorithm. The other was a partial derivative of RBF (PD-RBF) based strain estimation method which integrated denoising with differential process. The effectiveness and accuracy of the proposed methods were verified through two numerical simulation experiments. A practical application on the normal strain measurement of an aluminum alloy beam under symmetric four-point bending via an outer loading frame was also presented. Yue Gao, Teng et al. [29] focused on High-efficiency and high-accuracy digital image correlation for three-dimensional measurement. In which they used the three-dimensional DIC

(3D-DIC) which have its own importance over 2D. First, there were two cameras employed which increases the computational amount several times. Second, because of the differences in view angles, the must-do stereo correspondence between the left and right images is equivalently a non-uniform deformation, and cannot be weakened by increasing the sampling frequency of digital cameras. This work mainly focuses on the efficiency and accuracy of 3D-DIC. Because it contains the second-order displacement gradient terms, the measurement accuracy for the non-uniform deformation thus can be improved significantly. K.M. Saranath et al. [30] studied Zone wise local characterization of welds using digital image correlation technique. In which they studied the characterization of different zones such as fusion zone, heat affected zones and unaffected base material of a deposited weld was carried out using digital image correlation(DIC) technique. A methodology using the micrographic observation and image processing was proposed for accurate identification of various weld zones. The response of welded samples in the elastic and plastic region was compared with the original sample. Jinlong Chen et al. [31] studied Improved extended digital image correlation for crack tip deformation measurement and presented an improved X-DIC methodology to measure the discontinuous deformation across the crack. After simplifying the shape function of crack tip element based on the linear elastic fracture mechanics, non-rectangular subset was proposed to eliminate the effect of the crack width on the measurement accuracy. Then, the work verifies the performance of improved X-DIC by measuring the deformation of a specimen with a mode I crack. Experimental results show that the proposed method was effective at improving the measurement accuracy and enhancing the computational efficiency of X-DIC. Zhenyu Jiang, et al. [32] studied Path-independent digital image correlation with high accuracy, speed and robustness demonstrated that a path-independent DIC method was capable to achieve high accuracy, efficiency and robustness in full-field measurement of deformation, by combining an inverse compositional Gauss–Newton (IC-GN) algorithm for sub-pixel registration with a fast Fourier transform-based cross correlation (FFT-CC) algorithm to estimate the initial guess. In the proposed DIC method, the determination of initial guess accelerated by well developed software library can be a negligible burden of computation. The path-independence also endows the DIC method with the ability to handle the images containing large discontinuity of deformation without manual intervention. Furthermore, the possible performance of the proposed path-independent DIC method on parallel computing device is estimated, which shows the feasibility of the development of real-time DIC with high-accuracy. FeipengZhu et al. [33] focused on Measurement of true stress–strain curves and evolution of plastic zone of low carbon steel under uniaxial tension using digital image correlation

and they found that at certain time instant of expanding process of plastic zone, region that had already entered the plastic zone and that had not entered such zone yet was keeping in a constant deformed state, while region that was entering the plastic zone provides axial plastic deformation, which was almost equal to crosshead movement of testing machine. T.L.Jin. et al. [34] studied A study of the thermal buckling behavior of a circular aluminum plate using the digital image correlation technique and finite element analysis. In this study, the thermal buckling behavior of a circular aluminum plate that results from thermal loading was investigated using a digital image correlation (DIC) technique. The aluminum plate was placed in a titanium ring and the structure was heated from room temperature 25C to 160C. Due to the differences in the coefficients of thermal expansion (CTEs) between aluminum and titanium , the aluminum plate buckles at a certain temperature. The buckling temperature was determined from the full-field deformation shape and temperature-displacement curve that were obtained using the DIC- based ARAMISs .In order to verify the proposed measurement method, a finite element analysis of the structure was performed using the ABAQUS software. François Hild .et al. [35] studied Calibration of constitutive models of steel beams subject to local buckling by using digital image correlation .In which they focused on the behavior of steel beams prior to and after the inception of local buckling by using digital image correlation. Full-field measurements are used to evaluate kinematic and static fields for determining constitutive laws. It enables for the detection of local buckling inception and the evaluation of the post-buckled behavior. Constitutive models are tuned by using measured Euler Bernoulli kinematics. Fabienne Lagattu.et.al. [36] focused on High strain gradient measurements by using digital image correlation technique ,in which the efficiency of the digital image correlation method for measuring in-plane displacements in the presence of high strain gradient was discussed. Three types of strain gradient had been studied: strain localization around a hole in a composite laminate, strain concentration at a crack tip in a TiAl alloy, and strain gradient on a polymer neck front. These three applications concern various materials, various types of loading, and various gradient values. Results demonstrate the technique capabilities for a wide range of cases. Fabienne Lagattu.et al. [37] focused on In-plane strain measurements on a microscopic scale by coupling digital image correlation and an in situ SEM technique .And Presented a method based on the correlation of digital images obtained on a microscopic scale. A specific grainy pattern had been developed. The use of the scanning electron microscopy (SEM) allowed the determination of full field 2D displacements on an object surface with a spatial resolution of about 1 μ m. Validation tests were performed in order to quantify performances and limits of this method. An example of its application is presented for a Ti-6Al

4V titanium alloy. M. Koster. Et al. [38] studied Digital image correlation for the characterization of fatigue damage evolution in brazed steel joints and found that the heat treatment of brazed specimens had a significant influence on the fatigue damage evolution, especially under the influence of defects. Experiments with brazed defect-free specimens show that both heat treatments lead to comparable fatigue strengths for cyclic stresses below the yield strength of the base material. Under the influence of defects, brazed specimens with a better ductility provided higher fatigue lifetimes.

2.1 Research gap :

So far researchers have not done DIC analysis on crack propagation in Aluminum 1050 specimen under axial loading condition as well as on transverse loading condition. Moreover it had not been compared with numerical techniques.

2.2 Aim of the Study:

This study aims at the analysis of a specimens (with a crack and with or without hole) cantilevered from one side and under axial and transverse loading from other side , the crack propagation has been studied and points regarding accuracy have been considered for better results .and also aims at the modeling of the specimens in solidworks under different loading conditions and and results have been taken for comparison with that of DIC results

EXPERIMENTAL SETUP AND PROCEDURE

3.1 DIC setup

Digital image correlation technique setup has been used to take reading by capturing images of the deformed specimen under different loads . All the points regarding accuracy of the experiments have been kept in mind before doing experiments.

The experimental setup consists of :

- Digital Camera with flashes
- System containing DIC software
- White paint and markers
- Specimens.
- Universal Testing Machine.
- Software package SolidWorks
- Dead weights

3.1.1 Digital camera

A high resolution Digital Camera has been used with high end flashes. The camera has been attached to the CPU of the computer containing software .

The camera captured hundreds of images within fractions of seconds. which inturn compared by the software to get results. Following table gives the specification of the DIC camera

| S.NO | Specification | Value |
|------|---|--------------------|
| 1 | Pixel specification of camera (resolution) | 1024X1024 |
| 2 | Magnification | 3.25 μ m/pixel |
| 3 | Size of subset | 61x61 pixel |

Table 3.1 Table Showing specification of DIC camera



Figure 3.1 Setup containing various important component of DIC

3.2 Setup for crack growth propagation study :

This study has been done on two specimens under tensile load with the help of Universal Testing Machine (UTM) and DIC setup. Specimens have been cleaned properly before the application of load and due care has been taken of proximity from camera of DIC.

3.2.1 Specimen

For crack growth analysis two specimens have been made hard Aluminium 1050 , one specimen is with hole and crack and another without hole and with crack,

Both the specimens have been considered as cantilever from one side and tensile loaded from other side .

These two specimens are having following properties :

| S.NO | Specification | Value |
|------|---------------------------|--|
| 1 | Type (name) | Aluminium 1050 alloy |
| 2 | Young's modulus (E) | 71 GPa |
| 3 | Poisson's ratio (ν) | 0.33 |
| 4 | Density | $2.71 \times 10^{-006} \text{ kg mm}^{-3}$ |
| 5 | Total Length | 200mm |
| 6 | Grip length | 100 mm |
| 6 | Thickness | 2mm |
| 7 | Hole (specimen1) | 3mm |
| 8 | Slit width | 0.15mm |

Table 3.2 : showing properties of specimens used

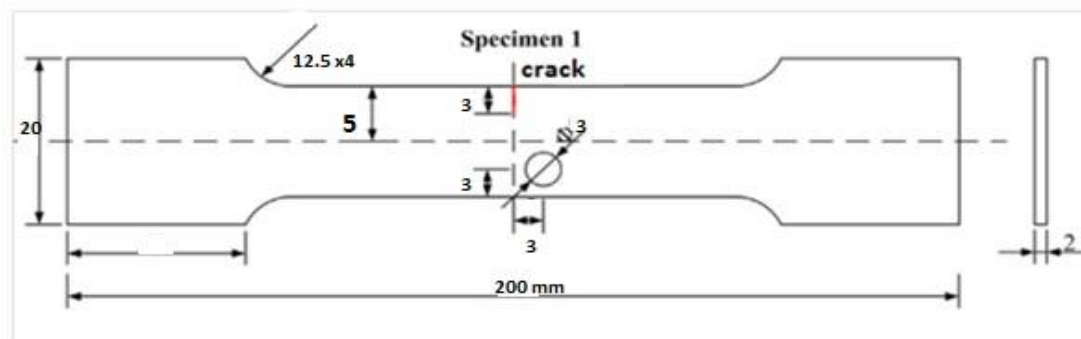


Figure3.2 :Specimen 1 with hole as shown in figure

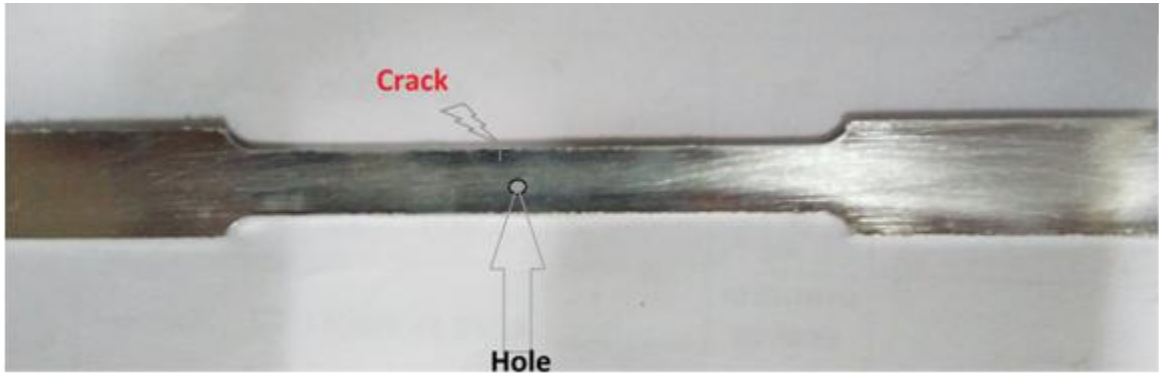


Figure3.3: Specimen 1 (with crack without hole)

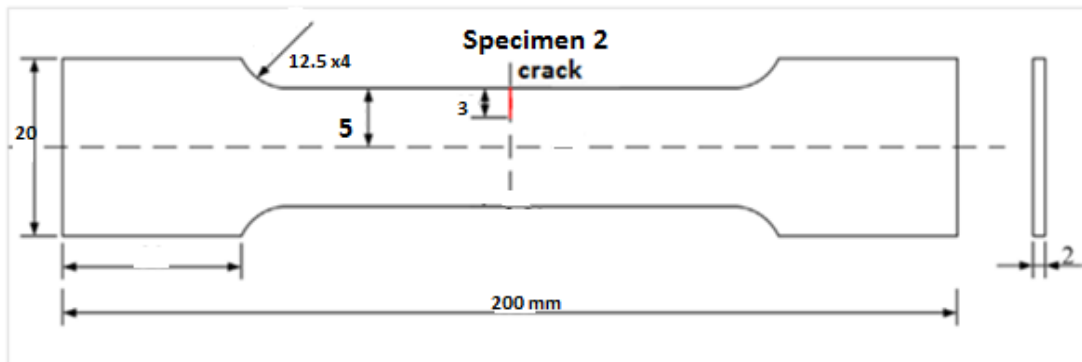


Figure3.4 : Specimen 2 without hole as shown in figure



Figure3.5 : Specimen 2 (with crack without hole)

3.2.1.1 Metallurgical study of specimen:

Metallurgical study has been done on the specimen and hardness number and type of grain has been analysed.

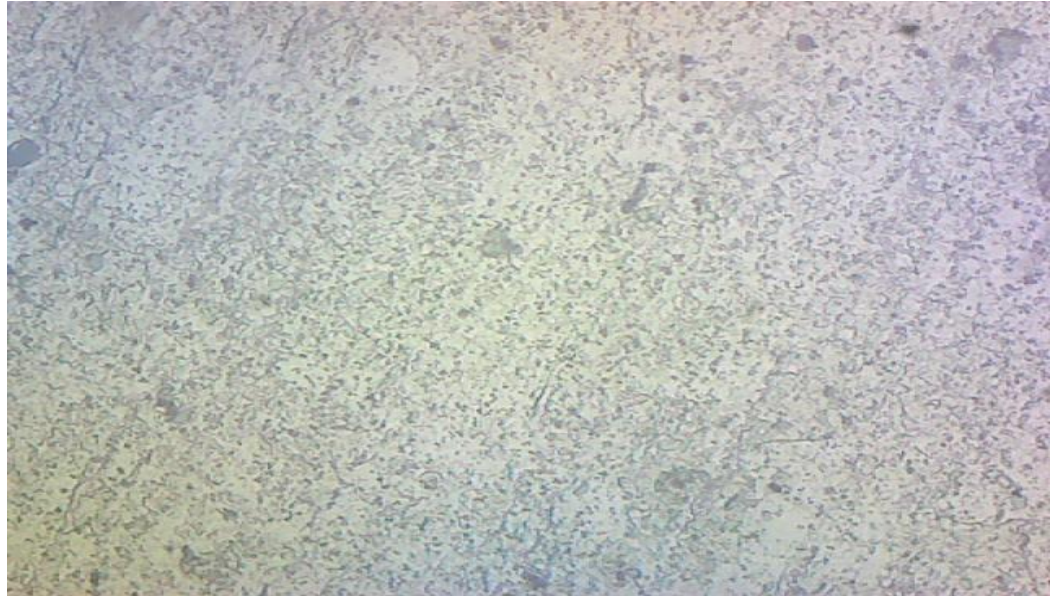


Figure3.6 : Specimen grain under testing

3.2.1.2 Composition of aluminium 1050

Aluminium 1050 is an alloy of aluminium with following composition

- Aluminium : 99.5% min
- Copper : 0.05% max
- Iron : 0.4% max
- Magnesium: 0.05% max
- Manganese : 0.05% max
- Silicon: 0.25% max
- Titanium : 0.03% max
- Vanadium: 0.05% max
- Zinc: 0.05% max

3.2.1.3 Brinell hardness testing on the specimen :

Brinell hardness number (BHN) is the measure of hardness of the material in which steel ball is used and indentation on the specimen is calculated by using the formula :

$$\text{BHN} = \frac{2P}{\pi D (D - \sqrt{D^2 - d^2})}$$

Where

P = applied force

D = diameter of indenter

d = diameter of indentation (mm)

following reading has been taken (time kept 20s):

- 1) Diameter for indentation : 3.37mm
- 2) BHN : 73.1436

Total length of the specimen has been taken as 200mm and width of the holder side has been taken as 20mm and the thickness as 2mm. Parallel length has been taken as 100mm.

With the help of wire EDM very thin slit of width .15 mm and 3 mm deep is cut on both the specimen at amidst from the both end , A small hole is made on specimen 1.

Diameter of hole = 3 mm (only in specimen 1).

3.2.2 Load specification :

Tensile force has been applied using UTM under displacement control and constant rate of 1mm /min. Force has been kept between 395N to 758N, according to the crack tip propagation and due care has been taken so that load act symmetrically on the both side of the crack , this has been done by making crack equidistant from both the side in both the specimen and thus mode I crack propagation can take place.

3.3 Universal testing machine :

A universal testing machine (UTM), is used to test the tensile strength and compressive strength of specimen . the name itself suggest that it can be use to load the specimen in any load according to its specification to check compressive and tensile stress as well as bending stress.

3.3.1 Components:

Conditioning - Sometime testing , requires conditioning such as humidity conditioning, pressure and temperature conditioning. The UTM machine is used to be kept in closed room for the minimal effect of the environment on the measurement,

Load frame – Usually comprise 2 bases for the machine we call them supports and some of the machines uses one also.

Load cell - It is used for measurement of the force that is going to be required. Calibrations are done timely for the quality of the machine.

Output device – It is a mean by virtue of which UTM provides the output in the form of the results o in way it is very important component of the UTM

Cross head – It is a part of UTM machine which can move up and down and also in constant speed and thus it is crucial component of the machine

3.3.2 Specification of available UTM machine:

| | |
|--------------|--|
| Name of UTM | H50KS |
| Capacity | 50KN |
| Test speed | Upto 25KN .001-500mm/min over 25KN .001-250mm/min |
| Jog speed | .001-500mm/min |
| Test area | Horizontal (between column) 405m Vertical 1100mm Depth unlimited |
| Return speed | .001-500mm/min |

Table 3.3: showing specification of UTM

3.3.3 Uses of UTM

The set-up and usage are detailed in a test method, often published by a standards organization. This specifies the sample preparation, fixturing, gauge length (the length which is under study or observation), analysis, etc.

The specimen is placed within the machine between the grips and an extensometer if needed will mechanically record the amendment in gauge length throughout the take a look at. If an extensometer isn't fitted, the machine itself will record the displacement between its cross heads on that the specimen is held. However, this technique not solely records the change in length of the specimen however additionally all different extending elastic elements of the testing machine and its drive systems together with any slipping of the specimen within the grips.

Once the machine is started it begins to use an increasing load on specimen. Throughout the tests the system and its associated software system record the load and extension or compression of the specimen. Machines vary from terribly small table top systems to ones with over fifty three MN (12 million lbf) capability



Figure3.7 :Universal testing machine

3.4 Experimental procedure of crack growth study on DIC :

3.4.1 Tensile loading :

UTM has been used for applying load on the specimen and specimens has been considered as fixed from one end and axially loaded from other end. Specimen has been loaded with proper care in the UTM so that no environmental effect can generate error in the study. Also it has been considered that the machine is placed in proper place where no environmental factor can affect the DIC camera images. DIC camera has been fixed in front of the UTM with all its accessories i.e. computer screen loaded with DIC software and two Flashes and all connection has been made as required by the DIC method. The Specimen 1 has been loaded on the UTM and load has been increase till the crack start propagating. Then load decreased to slow down the crack propagation, In the mean while DIC camera has taken thousands of images and on the software analysis of crack propagation has been generated. The displacement field(v) and the strain field(e) around the crack tip has been analyzed Similarly specimen 2 has been loaded on the UTM and images have been captured by the DIC camera . Analysis of the crack propagation has been done.



Figure3.8: UTM loaded with specimen

3.4.2 Transverse loading:

DIC camera with flashes and software package and computer system have been placed in front of the arrangement in which specimen is chucked by the vice from the one end.

For Transverse loading on specimen1, it has been placed on the vice from one side and from other side load has been gradually applied with the help of dead weight till the crack starts propagating. Images have been taken by the digital camera and thus it generates crack analysis on the screen according to the weight applied displacement field and strain field are studied.

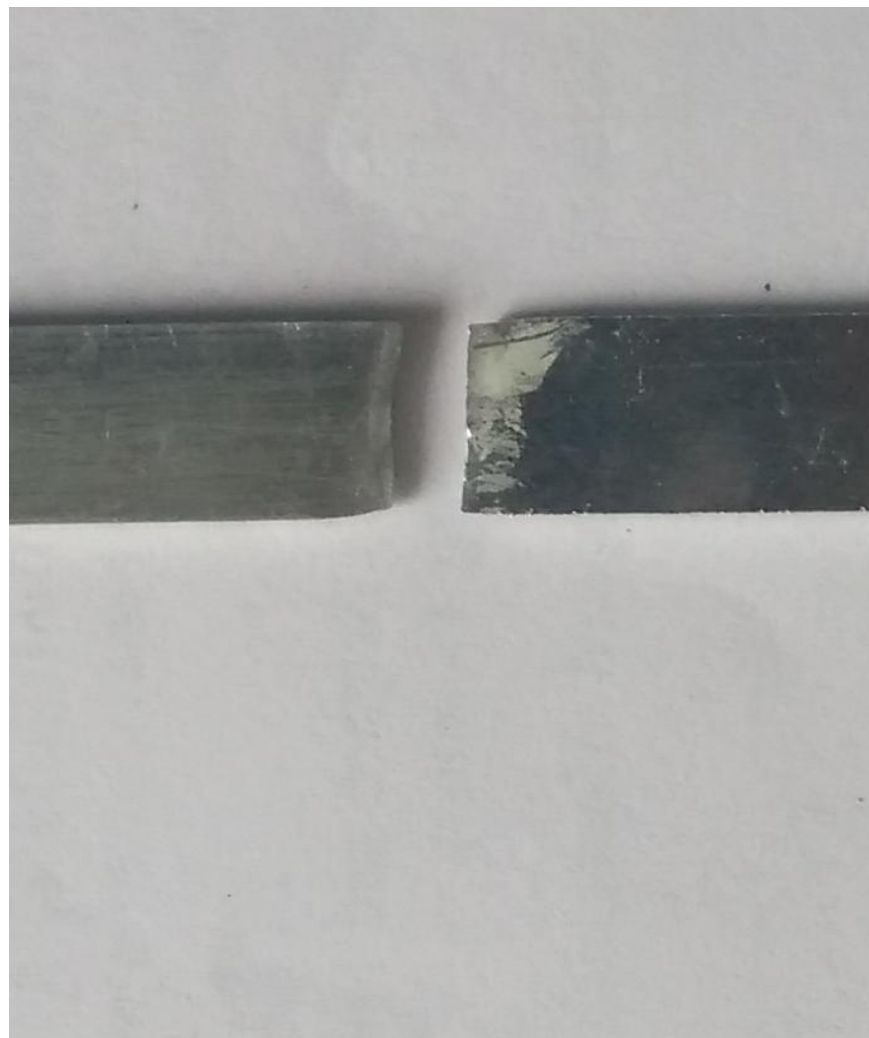


Figure3.9 : Specimen2 after loading

3.5 Procedure of crack growth study on software packages (Numerical Techniques)

For comparing the result from DIC technique which is quite an experimental technique some software packages is used which are as follows :

- 1) SOLID WORKS (for modelling and simulation)
- 2) ANSYS (for simulation)

Strain has been calculated at different point and at different load from the DIC software using its own algorithm , in the specimen and thus compared to the result shown by the software simulation results.

These packages require precise modeling of the specimen with the property input same as the specimen for the accurate results. Modeling has been done on solidworks and also reports has been generated by it . And also the model of the specimen that is made on the solidworks is imported in the ANSYS software.

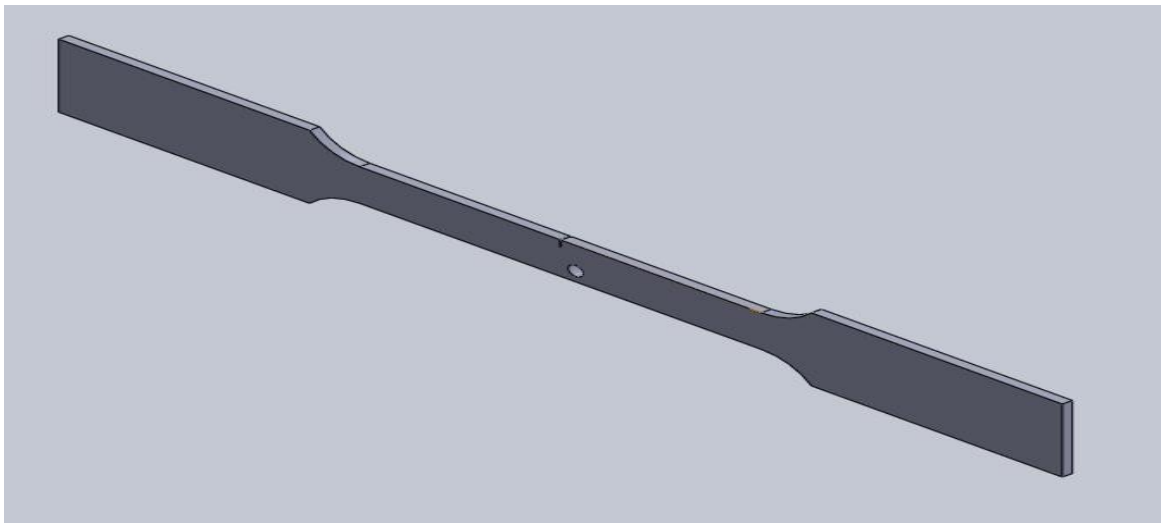


Figure3.10 : Showing model of Specimen 1 on SOLIDWORKS

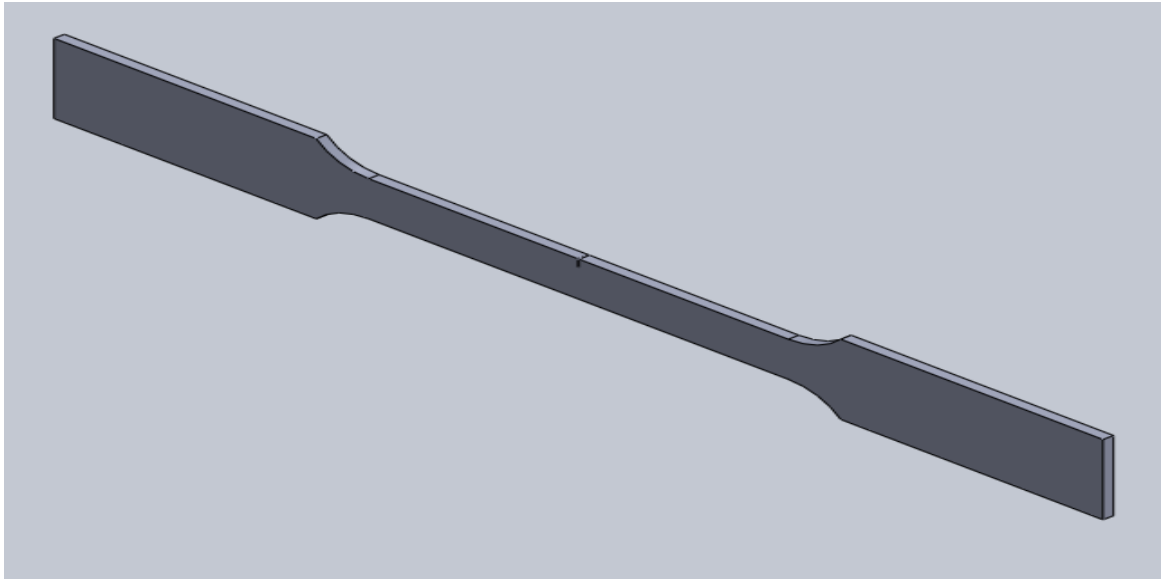


Figure3.11 : Showing model of Specimen 2 on SOLIDWORKS

3.5.1 Transverse loading :

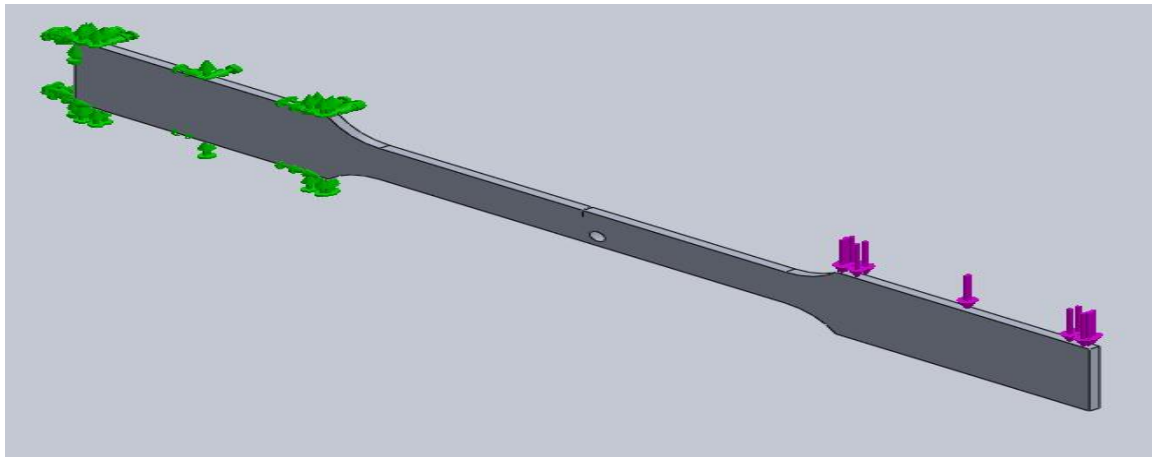


Figure3.12 : Showing Specimen 1 under transverse loading condition

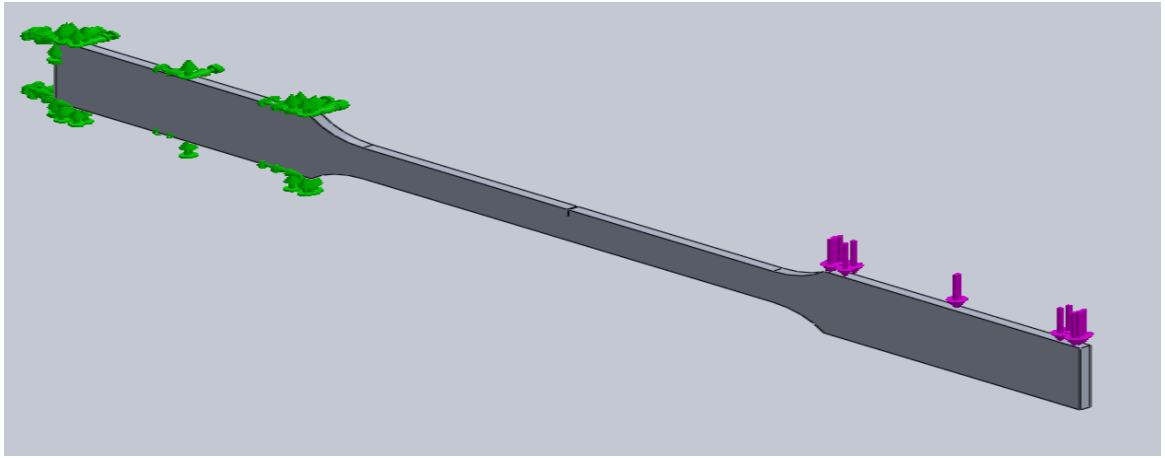


Figure3.13 : Showing Specimen 2 under transverse loading condition

Transverse load has been applied on both the specimens as shown in the figure . With different value of the load results have been taken into consideration and compared with the results of previously done DIC technique.

One side of the specimen has been kept fixed and load has been applied on another side , this has been done on both the specimens. The model then undergoes material selection in which all the valued of the properties of material has been given as input.

3.5.2 Tensile loading :

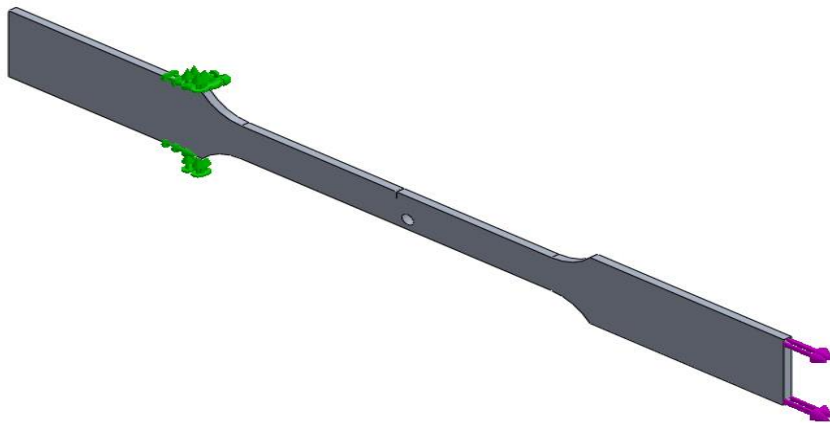


Figure3.14 : Showing Specimen1 under tensile loading condition

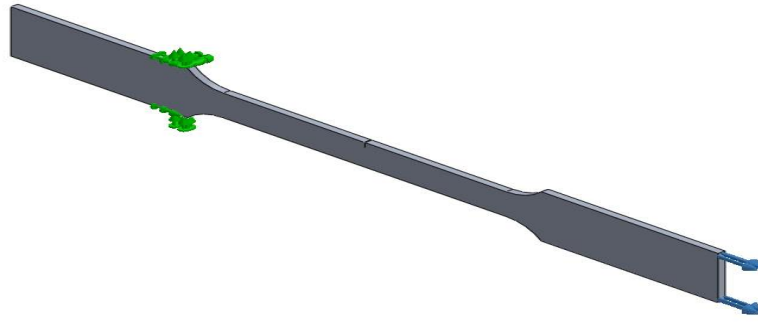


Figure3.15 : Showing Specimen 2 under tensile loading condition

Tensile load has been applied on both the specimens as shown in the figure . With different value of the load results have been taken into consideration and compared with the results of previously done DIC technique.

One side of the specimen has been kept fixed and load has been applied on another side , this has been done on both the specimens. The material selection has been done on the model in which all the valued of the properties of material has been given as input.

3.5.3 Material Properties

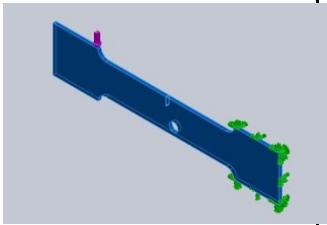
| Model Reference | Properties | Components |
|---|---|---|
|  | <p>Name: Aluminium 1050</p> <p>Model type: Linear Elastic Isotropic</p> <p>Default failure criterion: Max von Mises Stress</p> <p>Yield strength: 2.55e+008 N/m²</p> <p>Tensile strength : 2.9e+008 N/m²</p> <p>Modulus of elasticity : 71 e+009N/m²</p> | <p>SolidBody1(Cut-Extrude3)(Part1)</p> |

Table 3.4: showing properties of specimen modelled in SOLIDWORKS

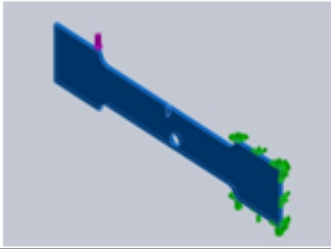
| Solid Bodies | | |
|---|-------------------|---|
| Document Name and Reference | Treated As | Volumetric Properties |
| Cut-Extrude4  | Solid Body | Mass:0.0193245 kg Volume:7.18382e-006 m ³ Density:2690 kg/m ³ Weight:0.18938 N |

Table3.5 : showing property of specimen taken

3.5.4 Fixture

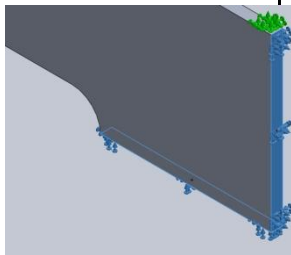
| Fixture name | Fixture Image | Fixture Details |
|--------------|---|---|
| Fixed-2 |  | Entities: 1 face(s) Type: Fixed Geometry |

Table3.6 : Showing Detail of fixture kept.

3.5.5 Load

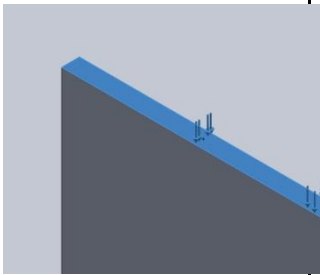
| Load name | Load Image | Load Details |
|-----------|--|---|
| Force-1 |  | Entities: 1 face(s) Type: Apply normal force Value: -225 N |

Table3.7 : Showing detail of force(transverse) applied.

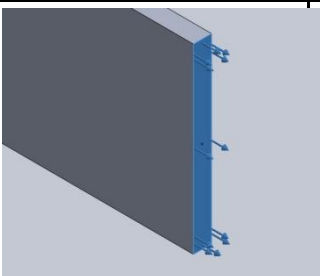
| Load name | Load Image | Load Details |
|-----------|---|---|
| Force-1 |  | Entities: 1 face(s) Type: Apply normal force Value: -758 N |

Table3.8 : Showing detail of force(tensile) applied.

One side of the specimen has been kept fixed to imitate the result of the cantilever beam under transverse load. And similarly to imitate the results of the specimen under tensile load one end is fixed and on other end (gripper) tensile load has been applied. Load has been varied from 395N to 758N and readings has been taken in all the loads and condition of both the specimen is compared with the condition of the specimen in DIC technique, like the elongation, the deformation is compared at every load.

3.5.6 Meshing :

Meshing is used to be done on the model made on SOIIDWORKS so that the accuracy of the result can be maintained. following figure shows that how meshing converges at the crack area.



Figure3.16 : Showing model of specimen 1 after meshing.



Figure3.17 : Showing model of specimen 2 after meshing

3.5.6.1 Mesh Information

| | |
|---------------------------------|---------------|
| Mesh type | Solid Mesh |
| Mesher Used: | Standard mesh |
| Automatic Transition: | Off |
| Include Mesh Auto Loops: | Off |
| Jacobian points | 4 Points |
| Element Size | 0.965147 mm |
| Tolerance | 0.0482573 mm |
| Mesh Quality | High |

Table 3.9 : Showing meshing information

After the load specification meshing is done on both the specimen. The quality of the mesh is kept high and it is taken care that irregular surface i.e. near crack and near circle it is done with high amount by taking fine mesh near hole and crack .

3.5.6.2 Mesh specification

| | |
|--|----------|
| Total Nodes | 99983 |
| Total Elements | 61745 |
| Maximum Aspect Ratio | 9.5159 |
| % of elements with Aspect Ratio < 3 | 99.8 |
| % of elements with Aspect Ratio > 10 | 0 |
| % of distorted elements(Jacobian) | 0 |
| Time to complete mesh(hh:mm:ss): | 00:04:08 |

Table 3.10 : Showing meshing specification

Total number of mesh nodes is kept 99983 which is near the maximum limit by the software. And total number of element is 61745 as shown in the table above. Aspect ratio of the element has been kept smaller than 3. The time taken by the software in generating mesh is 04 minutes and 8 seconds.

3.6 ANALYSIS USING ANSYS

ANSYS is also very reliable and mostly used modelling and simulation software used by designer. There are two methods to analyse in ANSYS , first one is to draw the model on the ANSYS software itself and then after meshing and different other steps analyses can be done by comparing with the results of experimental technique. Second method in which model part has been drawn on SOLIDWORKS and then it has been imported in ANSYS software has been applied in this project . After this all the property related to the specimens has been added in ANSYS. Tetrahedral , medium mesh has been generating using ANSYS itself and then analysis has been done by values of von mises stress and strain. All the specimens has been modelled in ANSYS and the analysis has been done after loading with different load. The report of ANSYS has been generated.

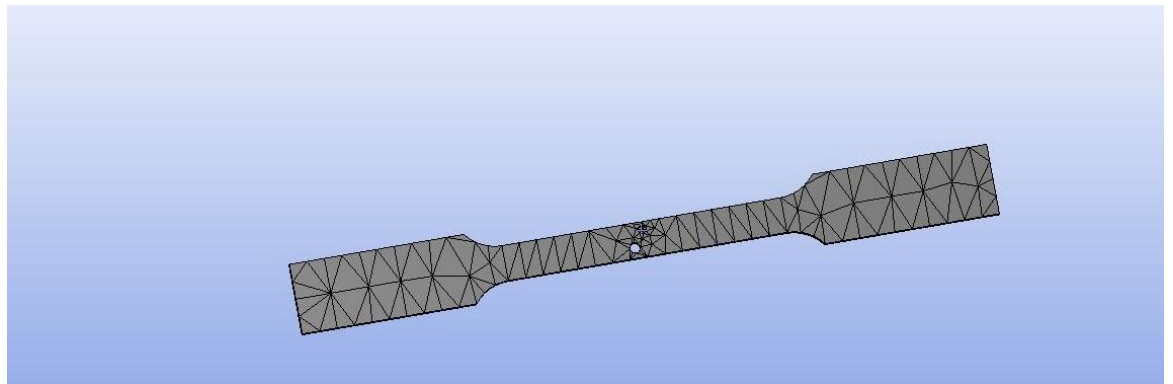


Figure3.18 : Mess generated in ANSYS

| | |
|-------------------|----------------------------|
| Object Name | <i>Geometry</i> |
| State | Fully Defined |
| Definition | |
| Source | H:\Part aluminium astm.IGS |
| Type | Iges |
| Length Unit | Meters |
| Element Control | Program Controlled |

| | |
|----------------------------------|------------------------|
| Display Style | Body Color |
| Bounding Box | |
| Length X | 200. mm |
| Length Y | 20. mm |
| Length Z | 2. mm |
| Properties | |
| Volume | 6105.3 mm ³ |
| Mass | 1.6545e-002 kg |
| Scale Factor Value | 1. |
| Statistics | |
| Bodies | 1 |
| Active Bodies | 1 |
| Nodes | 7634 |
| Elements | 2526 |
| Mesh Metric | None |
| Basic Geometry Options | |
| Solid Bodies | Yes |
| Surface Bodies | Yes |
| Line Bodies | No |
| Parameters | Yes |
| Parameter Key | DS |
| Attributes | No |
| Named Selections | No |
| Material Properties | No |
| Advanced Geometry Options | |
| Use Associatively | Yes |
| Coordinate Systems | No |

| | |
|-----------------------------------|------|
| Reader Mode Saves Updated File | No |
| Use Instances | Yes |
| Smart CAD Update | No |
| Compare Parts On Update | No |
| Attach File Via Temp File | Yes |
| Analysis Type | 3-D |
| Mixed Import Resolution | None |
| Decompose Disjoint Geometry | Yes |
| Enclosure and Symmetry Processing | Yes |

Table3.11: Showing procedure and inputs to ANSYS

RESULTS AND DISCUSSIONS

4.1 Results of DIC analysis of crack tip propagation on Tensile loaded specimen:

Digital camera of Digital image correlation technique has taken images as input and provided to the software attached to it, which in turn has given the results of the crack tip propagation. Following are the processed images captured by DIC and the propagation of crack has been shown in them. The specimen1 is loaded on UTM and images has been captured by DIC camera.

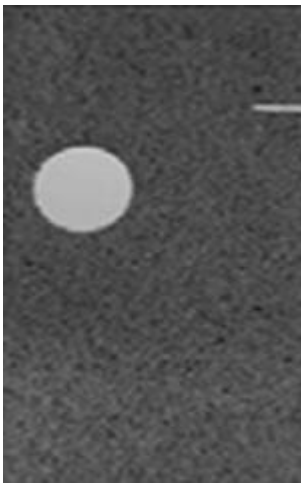


Figure 4.1: specimen 1 at F=545N

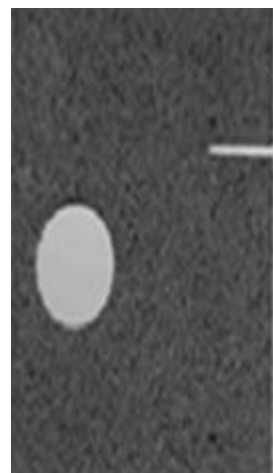


Figure 4.2 : specimen 1 at F=732N

Figure 4.1 shows the specimen 1 being loaded with 545 N, the elongation has been observed near slit but the crack has yet not observed at this point. Figure 4.2 is the processed image of the specimen1 when load has reached to maximum(732N). At this condition crack started propagating and crack propagation can be divided into following steps. First when the load reaches to maximum value i.e. 732N then unstable crack propagation is depicted. then, the crack propagation stopped when load decreased or reaches to 395N the phenomenon can be depicted by the image in the figure 4.3, gradually the crack propagation changed from the transverse direction to the direction towards the hole. When the direction of the propagation curves towards hole at

certain angle then the crack growth stopped. Finally load is again increased to 410N and then the crack started propagating towards the hole. Figure 4.4 shows the condition of the specimen at this load .

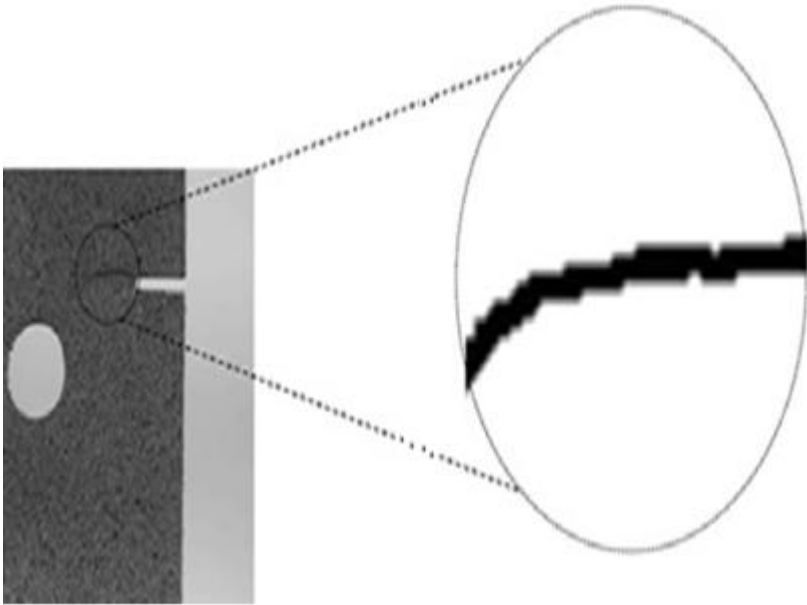


Figure 4.3: Showing specimen 1 at load 395N and the crack .

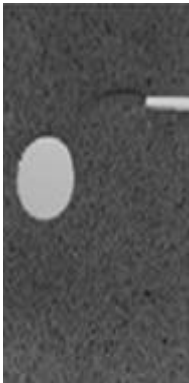


Figure 4.4: Showing Specimen 1 at load 410N and the condition of crack at this load.

Now the load is increased and it has been observed that the crack propagates through hole after curving towards hole with the increase in the load. Figure 4.5 shows the condition at load equals to 445 N .

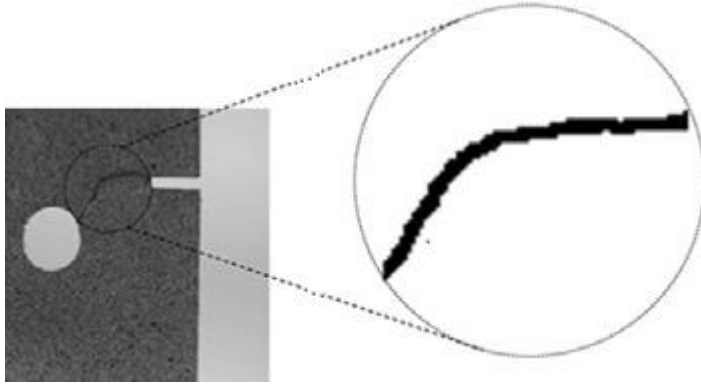


Figure 4.5 : Shows the condition when crack propagates through hole.

The same thing has been repeated on the specimen 2 and figure 4.6 shows the processed image of specimen 2 under a load of 545N . The elongation of the specimen has been observed near slit but no crack is observed. Thus the load has been gradually increased and at the value of 758N crack has been observed near slit thus this is termed as the crack starting point and this point is depicted in Figure 4.7 . Then the load is decreased to 395 N and after this it has been increased gradually to 410N. In the loading condition of specimen 2 the crack goes straight without curving anywhere, when the load being increased further.

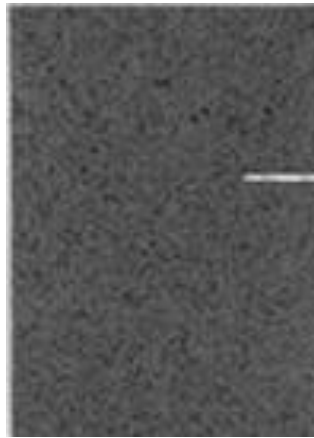


Figure 4.6 : Specimen 2 under 455N

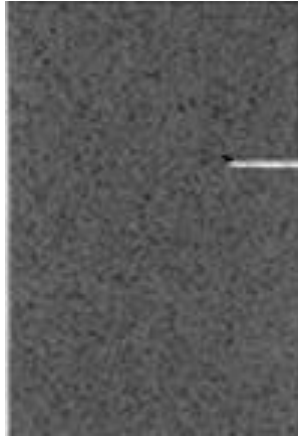


Figure 4.7: showing processed image of the specimen2 at load 758N.

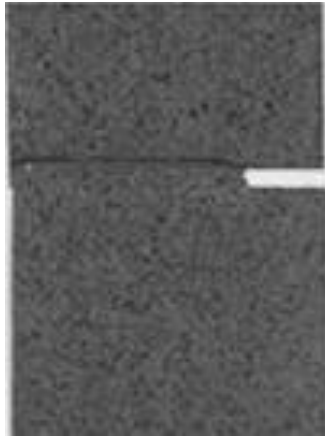


Figure 4.8 : Showing processed image of specimen 2 having straight load.

Figure 4.8 shows that the crack propagates straight in transverse direction towards the other end of the specimen2 ,but figure 4.5 shoes that if there is a small hole in the proximity of the crack then the crack propagates in such a manner that it will pass through it. There is curving of crack towards the hole. The presence of hole has decreased the load requires to generate crack propagation this can be seen from the results.

4.2 Displacement field and strain field near crack tip :

Images of the displacement field and strain field near crack tip have been taken from the software which depicted the fields generated around the crack tip in different loading conditions.

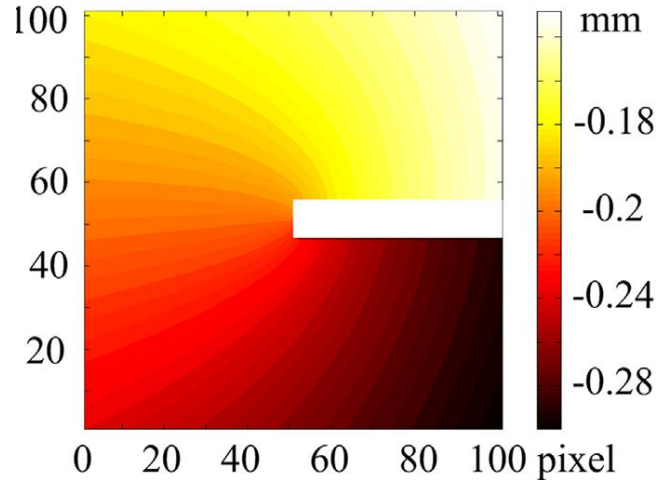


Figure 4.9 Image showing v field in specimen 1 under the loading condition between 545N to 732N

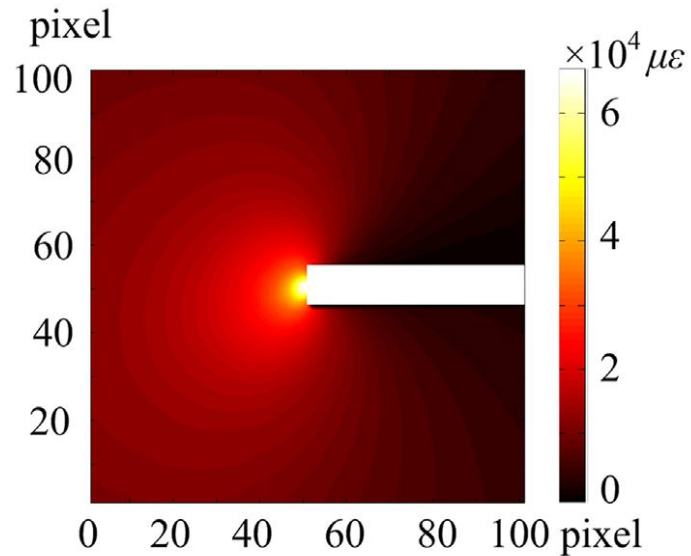


Figure 4.10 Image showing the E field specimen1 under the load between 545N to 732N

Figure 4.9 shows the displacement field (v) and which is near symmetric about the crack tip when the load has been increased from 545 , it then started curving towards longitudinal direction. The strain field (e) is shown in the figure 4.10, it has shown in the image that strain field is somewhat symmetric about the crack tip, until the load has been increased to maximum value.

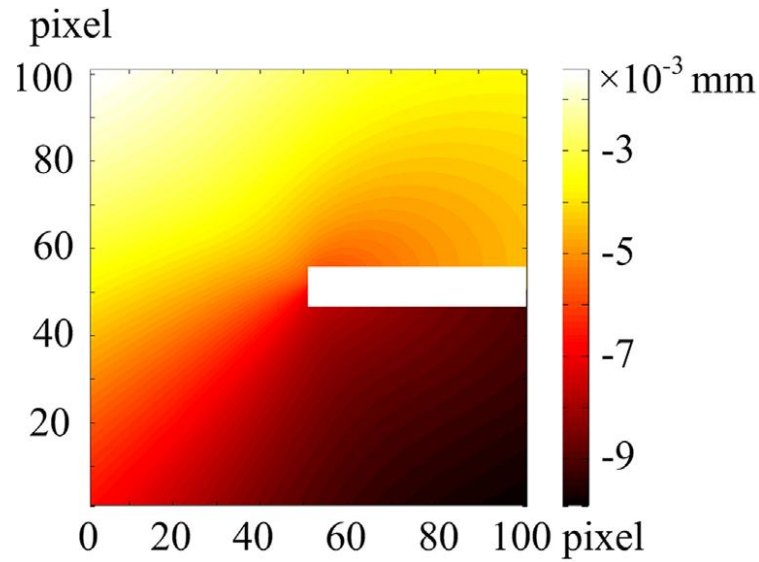


Figure 4.11 Image showing v field in specimen 1 when the load 395N to 450N

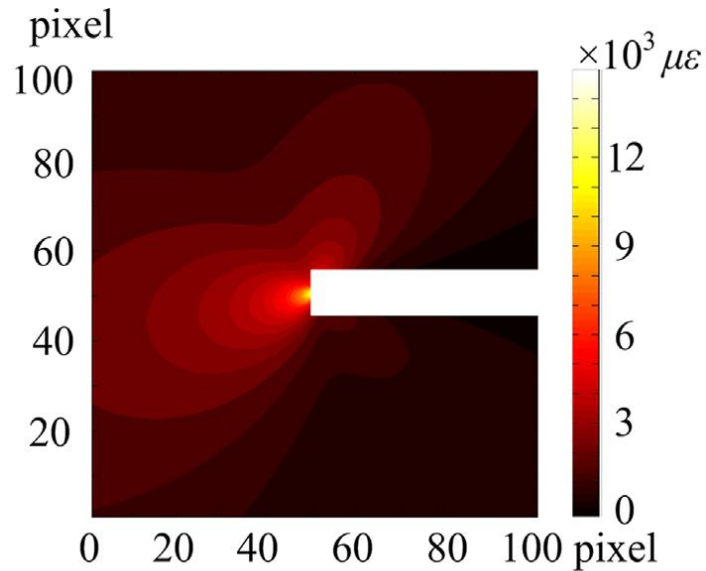


Figure 4.12 : Image showing e field in specimen 1 between the load 395N to 410N

The displacement field as shown in the figure 4.11 depicts that displacement field converges towards the hole when crack propagation starts. When the load has increased from 395N to 410N it has started converging more and more towards the hole. Strain field as shown in figure 4.12 clearly depicts the distorted field around the crack tip.

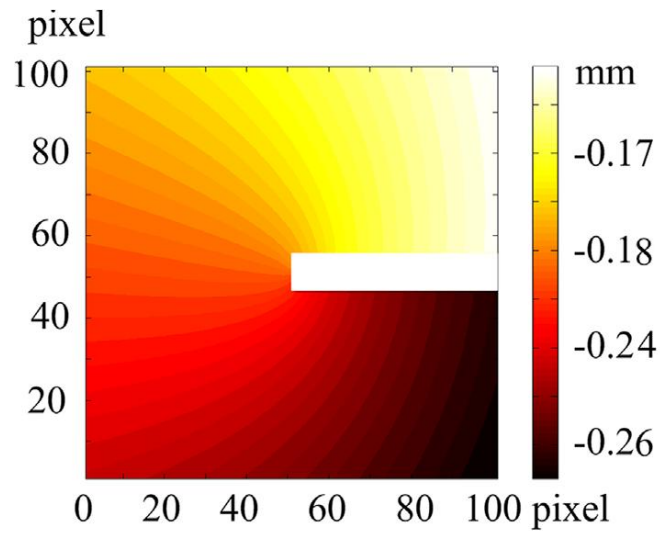


Figure 4.13 : Image showing v field in specimen 2(without hole) under load 545N to 758 N

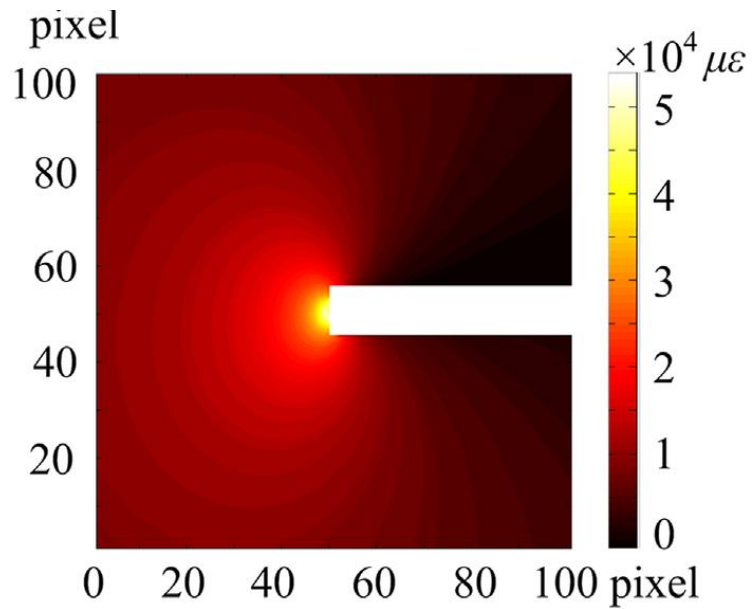


Figure 4.14: Image showing distribution if e field in specimen 2 (without hole) under load 545 N to 758 N

Figure 4.13 and figure 4.14 are showing the v fields and e fields around crack tip in specimen 2. It has been clearly depicted by these images that when there is no hole in the proximity of the crack the displacement field and strain field remains symmetric around the crack tip. Thus the crack has propagated in transverse direction without curving in the longitudinal direction.

4.3 Result of the UTM machine in crack tip propagation study of tensile loaded specimen :

UTM machine has provided graph between load and deformation of specimen 1 and specimen 2 under tensile test .

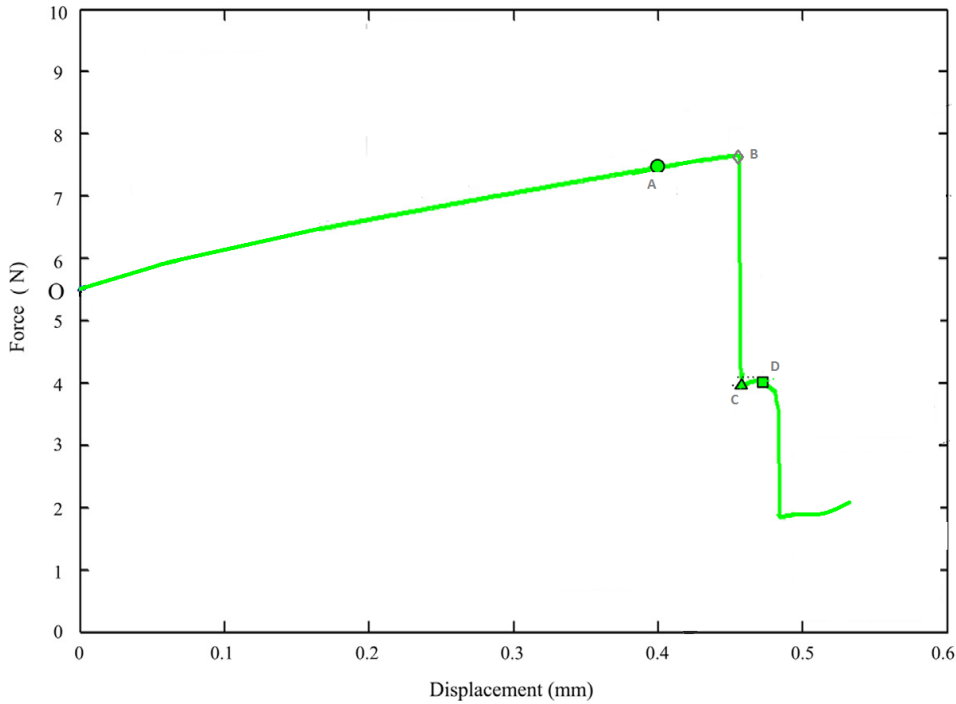


Figure 4.15 : Showing Graph between Force and displacement in specimen 1

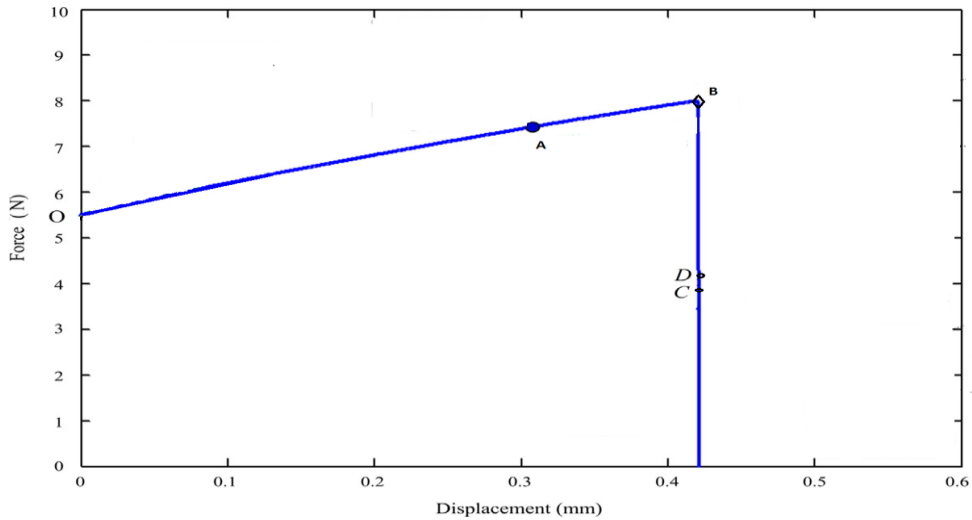


Figure 4.16 : Showing graph between load and displacement in specimen 2

These results clearly depict the relationship between load and deformation in both the specimens , on comparing these results it can be concluded that certain higher load has been applied on the specimen 2 to generate crack propagation . Moreover these results have helped in comparison of the results from DIC and real time results.

Loads are depicted by A,B,C,D

4.3.1 For specimen 1 :

| POINT | LOAD |
|--------------|-------------|
| O | 545N |
| A | 710N |
| B | 732N |
| C | 395N |
| D | 410N |

4.3.2 For specimen 2:

| POINT | LOAD |
|--------------|-------------|
| O | 545N |
| A | 732N |
| B | 758N |
| C | 395N |
| D | 410N |

4.4 RESULTS OBTAINED FROM SOLIDWORKS:

After detailed modeling the result has been discussed below

4.4.1 Results for Specimen1 under tensile load :

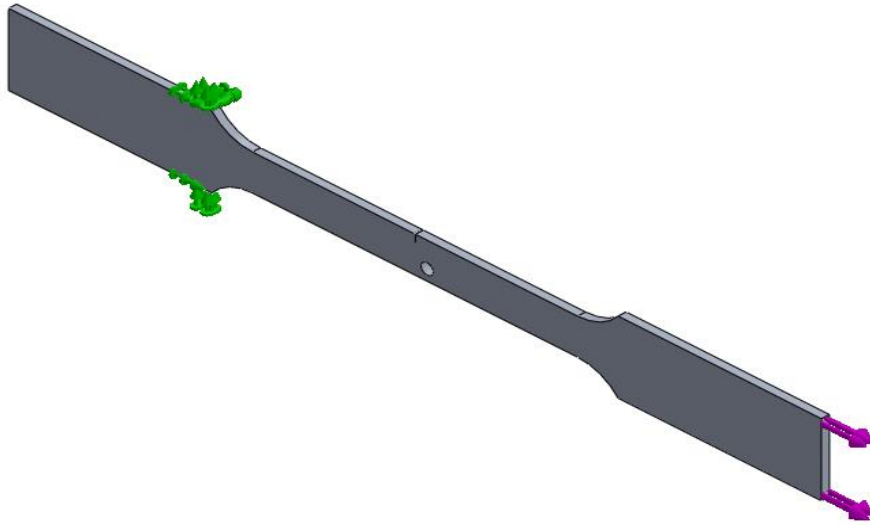


Figure 4.17 Showing tensile load applied on specimen 1

Figure 4.17 and figure 4.18 is showing how the load has been applied on the specimen1 and specimen2 respectively. Strain results and stress results have been taken from solidworks, and these results have been compared with that of results shown by DIC and UTM. Figure 4.19 clearly depicts the direction of propagation of crack in the specimen 1 which is longitudinal in direction towards the hole.

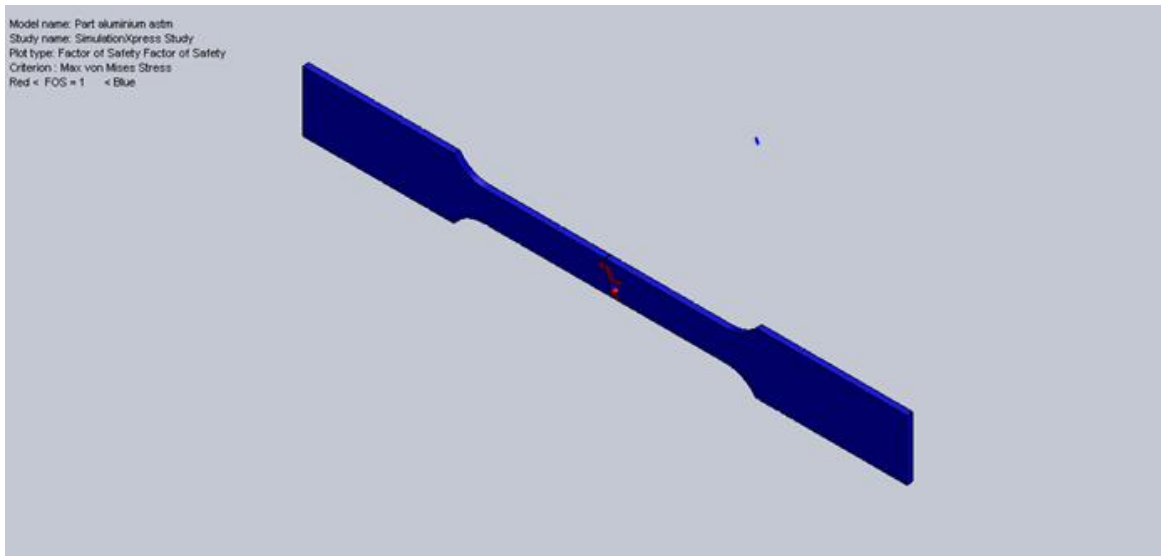


Figure 4.18 Showing final state of the specimen when maximum loading ($F=760N$) has been done in specimen 1

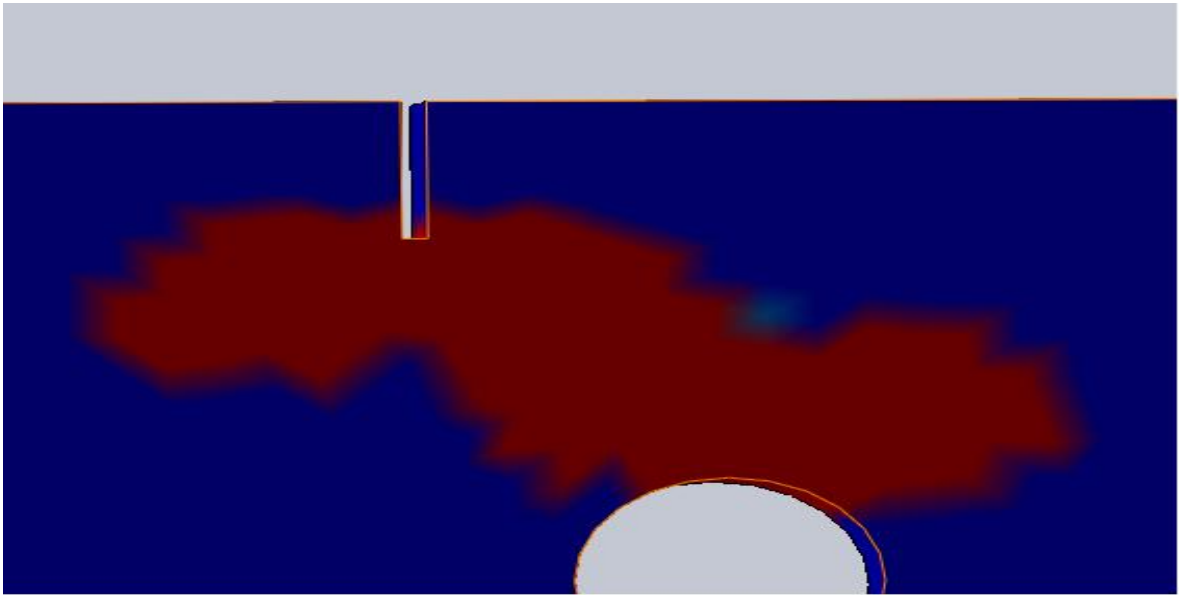


Figure 4.19 Showing zoomed image of final state of the specimen1 when maximum loading ($F=760N$) has been done in specimen

Figure 4.18 is showing the specimen when loading has been done , red area is showing the elements having factor of safety smaller than one which in turn implies that material will fail accordingly from this area thus this validates the results shown by DIC in which material has been failed by crack , there is small difference in the value of load which is in the range of 97.8%

accuracy. This difference in the results are due to assumption taken by solidworks in its algorithms.

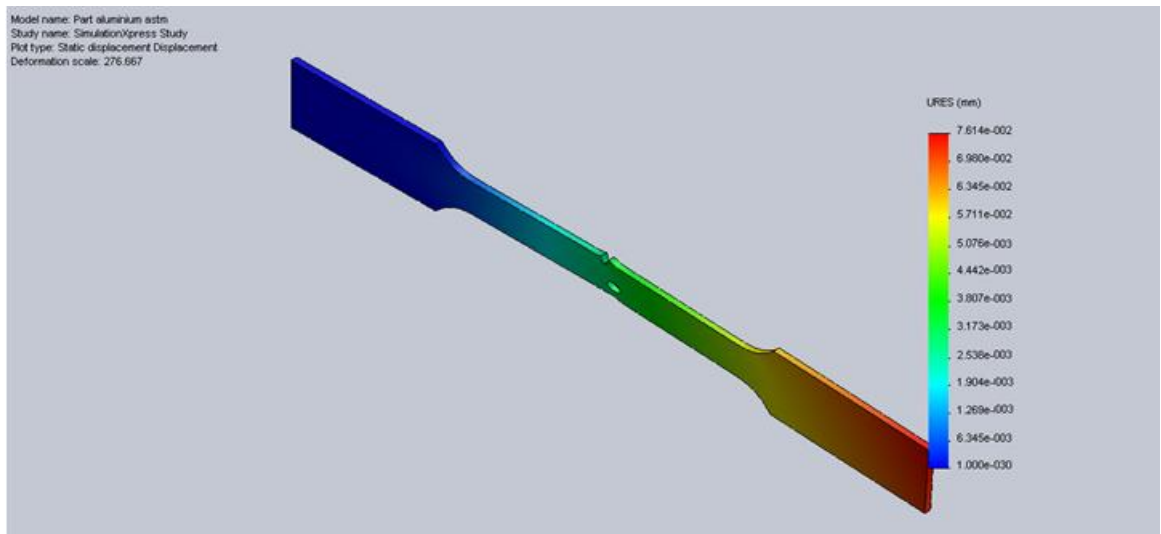


Figure 4.20 showing displacement in the specimen 1 at different points.

Displacement has been shown by the software as shown in figure 4.19,

Maximum displacement = $7.614e-002$

Minimum displacement = $1.000e-03$

At the crack tip = $2.64e-003$

Around the crack tip strain measured by DIC has been in the range of $17e-002$ to $26e-002$ (from figure 4.9)so its shows that range of strain measured by DIC and SOLIDWORKS are approximately equal around the crack tip within the error of 2%.

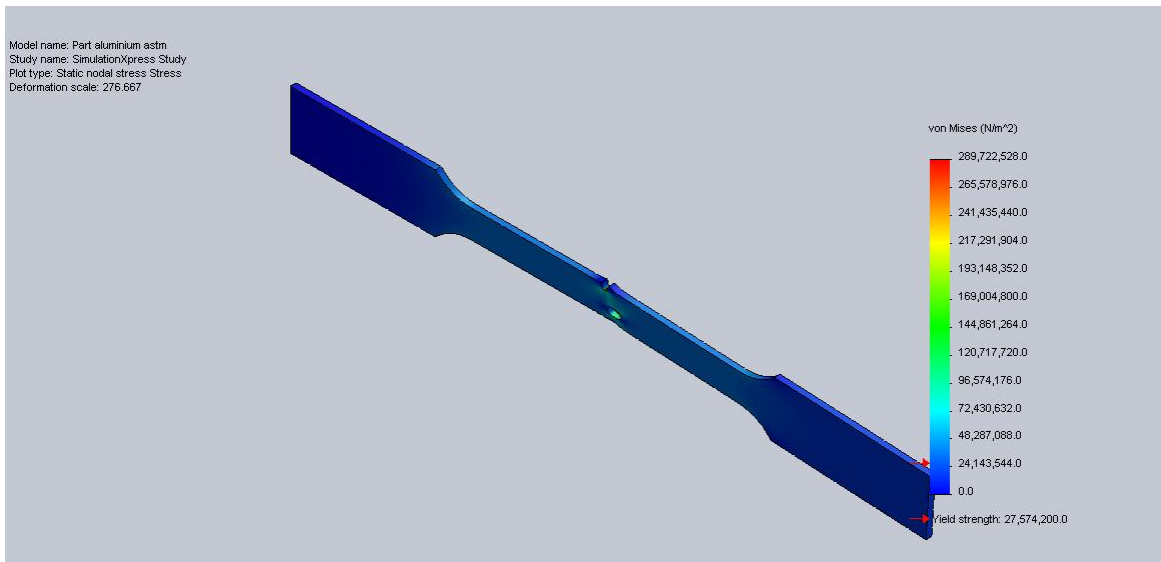


Figure 4.21 showing stress(von mises) at different point in the specimen 1

Von mises stress has been shown by the figure 4.21 , it has been shown in the figure 4.22 that maximum stress has been induced in the slit tip area , which is greater than the yielding stress of aluminium 1050 (275MPa). Thus it can be clearly understood from this result that crack propagation started at the slit end of the specimen.

At slit end stress has been found as 289 MPA which indicates crack has been formed at this point at slit end

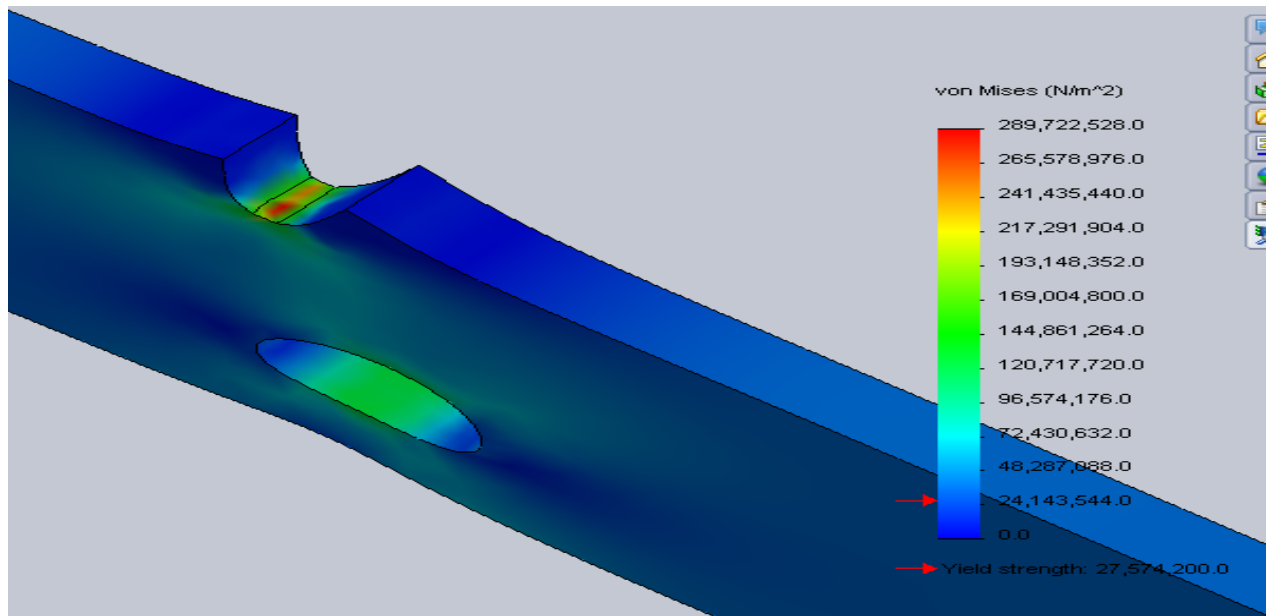


Figure 4.22 Showing crack tip area at the load of 760 N

4.4.2 Results for Specimen 2 under tensile load :

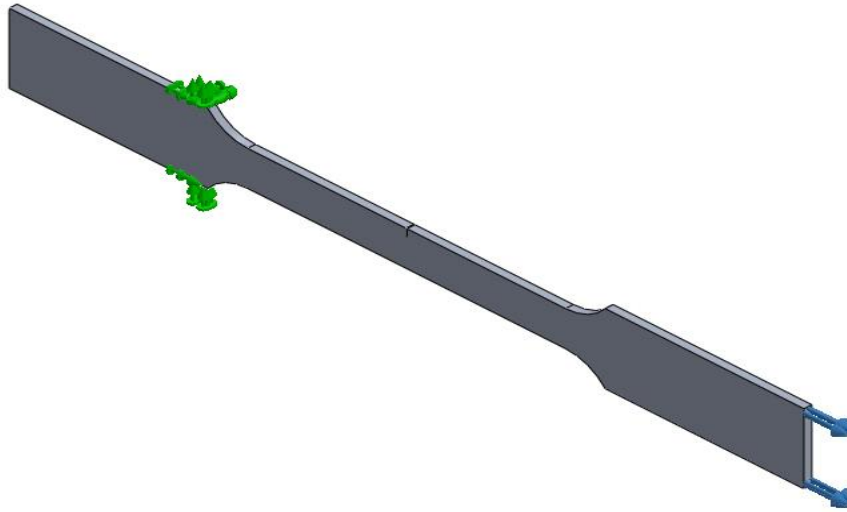


Figure 4.23 Showing tensile load applied in specimen2.

Specimen 1 has been modeled in solidworks as shown in the figure 4.23 analysis of the stress , strain is done on the solidworks and results into results depicted by image shown in the figure 4.24.

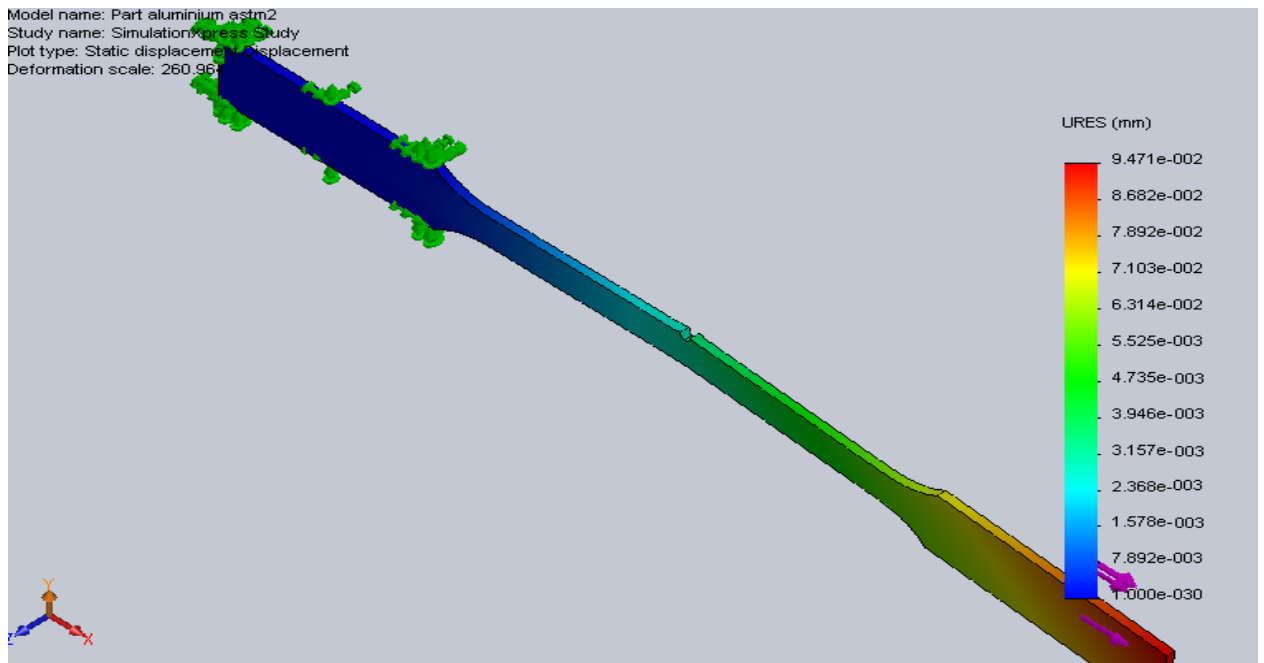


Figure 4.24 Showing displacement produced in the specimen2 on tensile loading at load equals to 758N

Displacement has been shown by the software as shown in figure 4.19,

Maximum displacement = $9.471e-002$

Minimum displacement = $1.000e-03$

At the crack tip = $2.64e-003$

Around the crack tip strain measured by DIC has been in the range of $17e-002$ to $26e-002$ (from figure 4.13) so it shows that range of strain measured by DIC and SOLIDWORKS are approximately equal around the crack tip within the error of 2%.

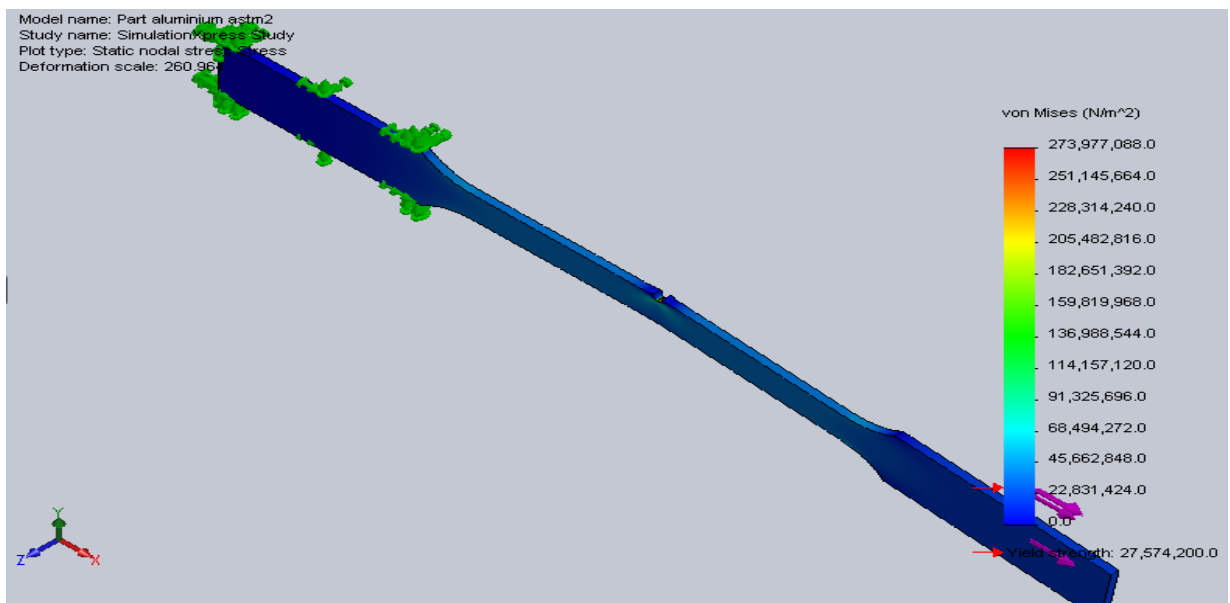


Figure 4.25 Shows the von mises stress in specimen2 under tensile load of 758N

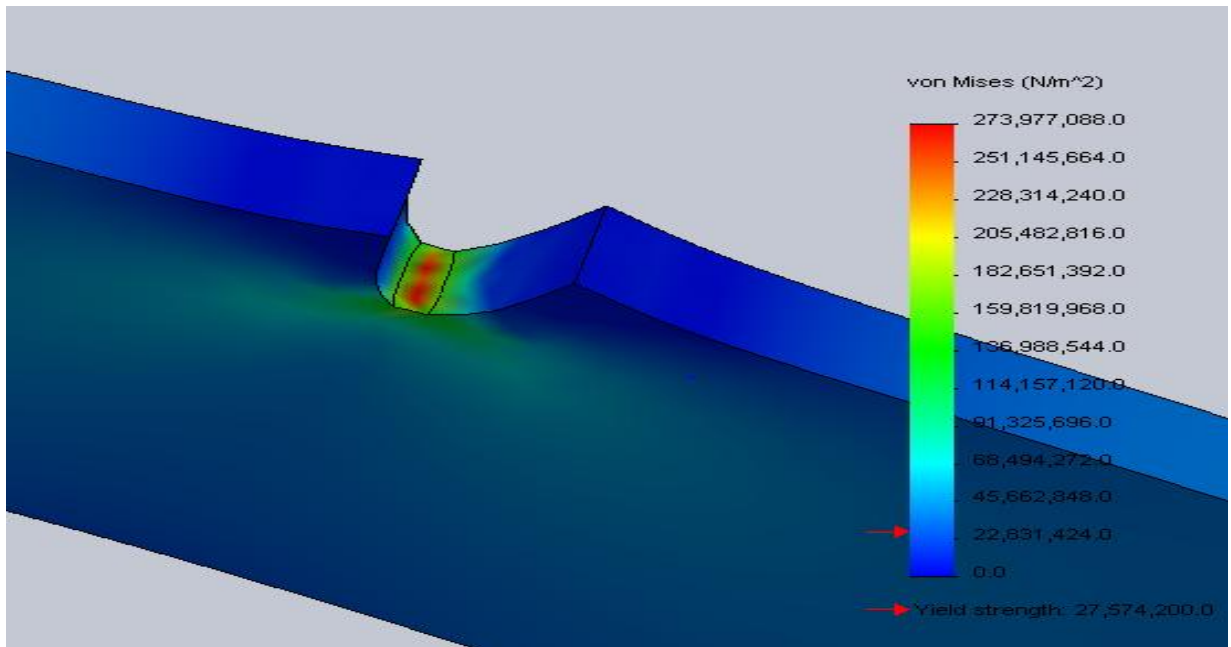


Figure 4.26 Shows the von mises stress in specimen2(near slit end) under tensile load of 758N

Von mises stress has been shown by the figure 4.25 , it has been shown in the figure 4.26 that maximum stress has been induced in the slit tip area , which is greater than the yielding stress of aluminium 1050 (275MPa). Thus it can be clearly understood from this result that crack propagation started at the slit end of the specimen.

At slit end stress has been found as 276 MPa which indicates crack has been formed at this point at slit end.

4.4.3 Transverse loading results in specimen 1:

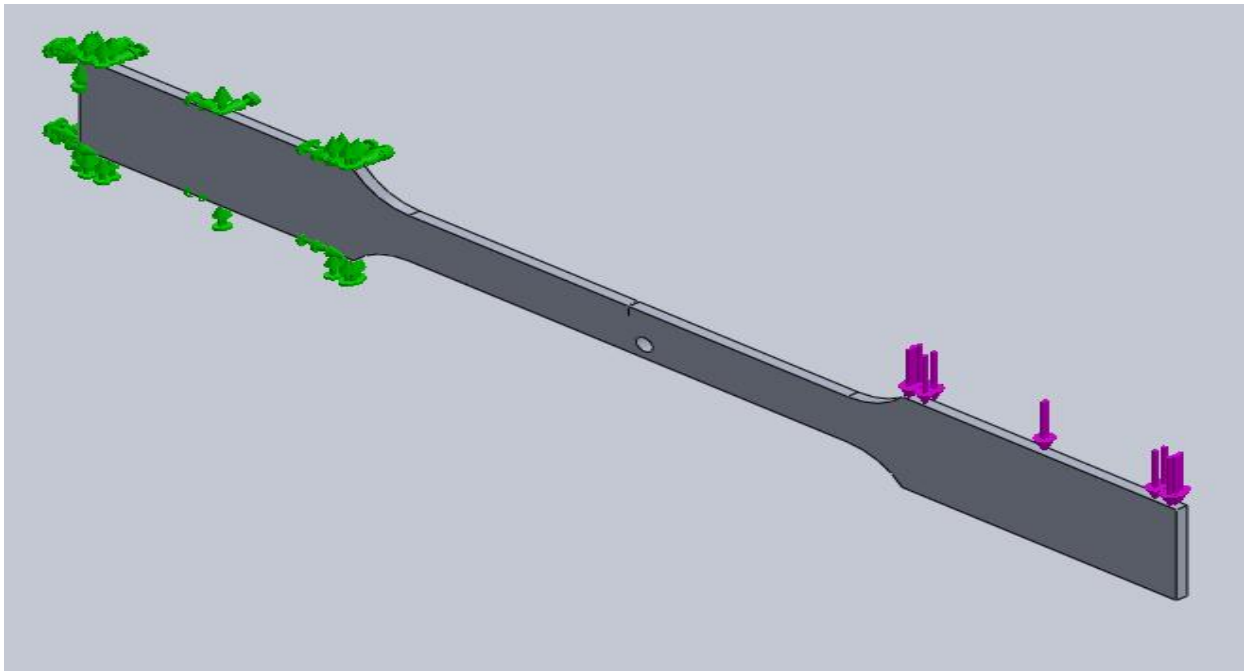


Figure 4.27 : Showing Specimen 1 under transverse loading condition

Figure 4.27 shows that how modeling of transverse loading in the specimen has been done . In this case bending of the specimen has been observed, load of 225N has been applied on the free end of the cantilever . Figure 4.28 and 4.29 are showing the stress and displacement in the specimen1.

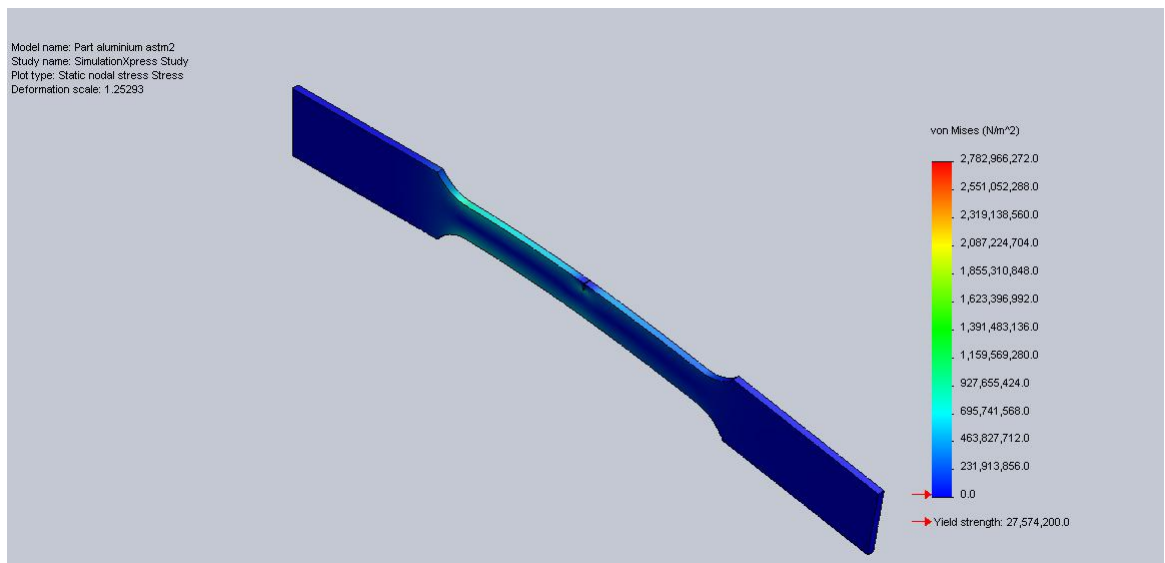


Figure 4.28 showing von mises stress in specimen 1 under transverse loading.

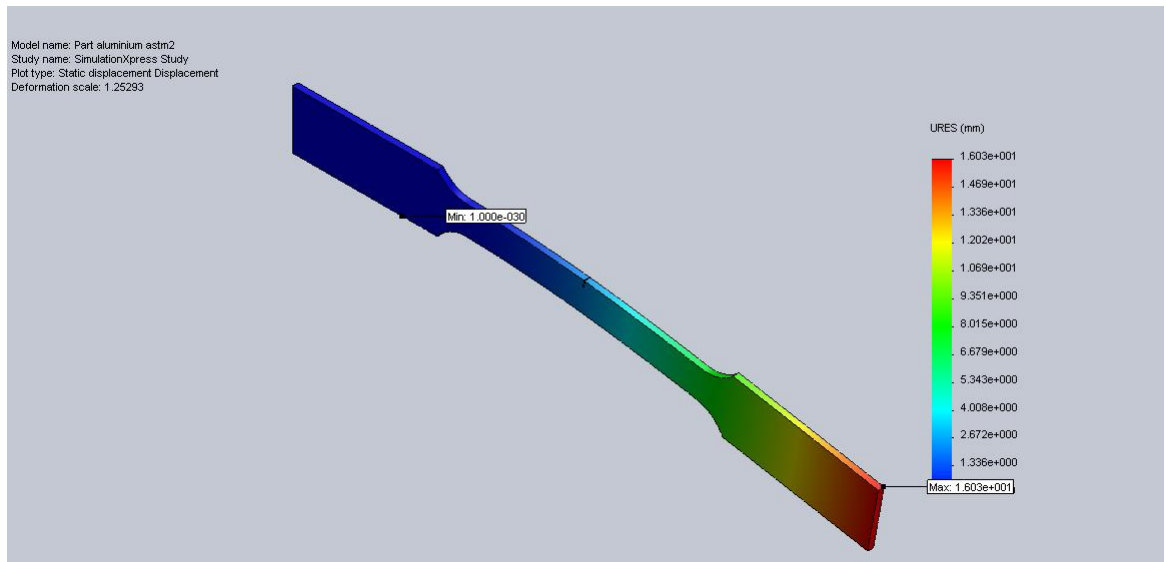


Figure 4.29 showing displacement in specimen 1 under transverse loading.

Displacement has been shown by the software as shown in figure 4.19,

Maximum displacement = $1.603e+001$

Minimum displacement = $1.336e+000$

At the crack tip = $2.64e+000$

4.4.4 Transverse loading results in specimen 2:

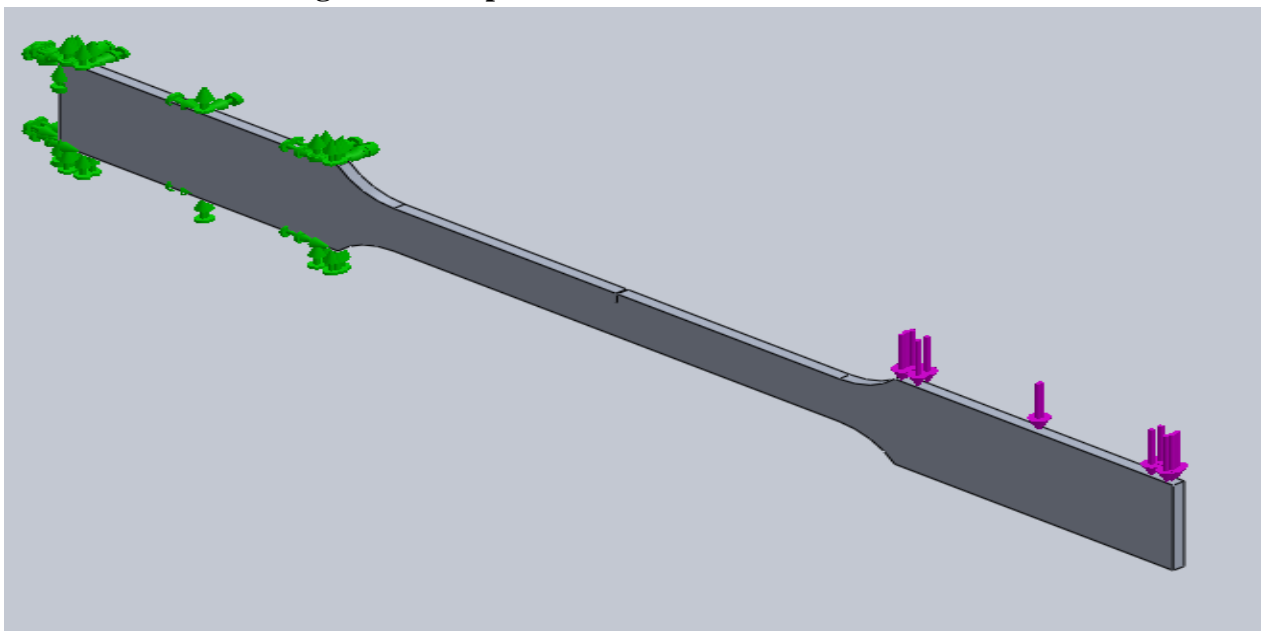


Figure4.30 : Showing Specimen 2 under transverse loading condition

Figure 4.30 shows that how modeling of transverse loading in the specimen2 has been done . In this case bending of the specimen has been observed, load of 225N has been applied on the free end of the cantilever . Figure 4.31 and 4.32 are showing the stress and displacement respectively in the specimen2, at the slit end stress induced has been found to be more then yielding stress of aluminium 1050 so crack generated from here .

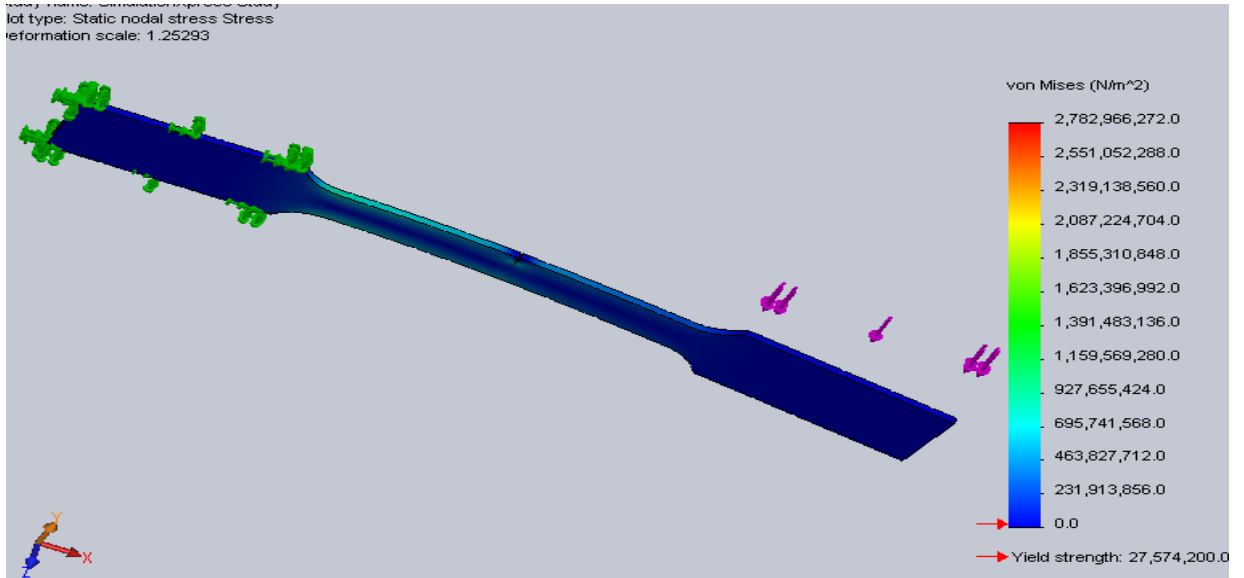


Figure 4.31 showing von mises stress in specimen 2 under transverse loading.

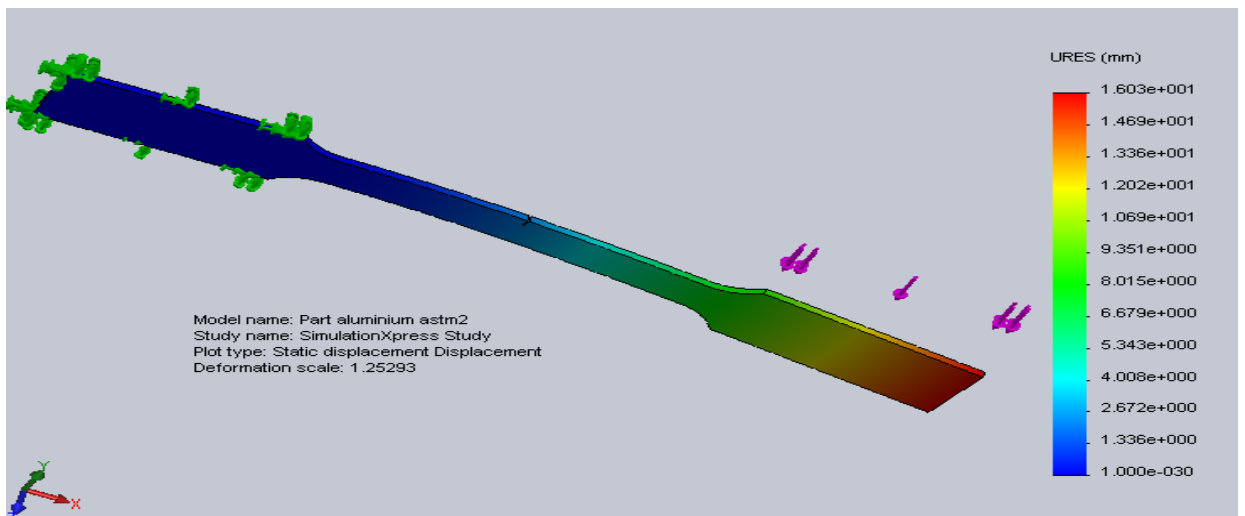


Figure4.32 : Showing Specimen 2 under transverse loading condition

Displacement has been shown by the software as shown in figure 4.19,

Maximum displacement = $1.603e+001$

Minimum displacement = $1.336e+000$

At the crack tip = $2.64e+000$

Conclusion and further scope of the study

From the study of the two specimens (one with hole and one without hole) using DIC technique and further comparing results with that of numerical technique like SOLIDWORKS and ANSYS it can be concluded that if the hole is present within certain proximity to the crack then crack tends to propagate in the direction such that it passes through it i.e. in case of the specimen selected for this study the specimen 1 in which hole is there the crack has been found propagating first in transverse direction then curving in longitudinal direction. And in case of specimen 2 which is not having hole it propagated in transverse direction only. It can be further concluded from the results that crack propagates in the direction of displacement fields and strain field formed around crack tip by DIC software using its own algorithm ,before propagating in real time.

In this study specimens are considered as cantilever from one side and axial load is applied on other side , the mass of specimen was less compared to the real time beam present in day to day activities so this study require larger specimen and latest techniques to apply transverse loads on bigger specimen to get real time results. Further as there was paucity of time as well as proper equipment for application of transverse force on the specimen study restricted itself to axial loads only but it can be applied efficiently in transverse loaded cantilever beam.

DIC has tremendous scope in detecting strain and cracks in practical application that too in working condition of the products and machines. And also it is having an edge over other contemporary techniques as far as time, economic, and simplicity is concerned. It can be further applied in real time study of the products working on different loads acting at a time like in shafts, beams etc.

REFERENCES

- [1] Peters WH et al. “Digital image techniques on experimental stress analysis”. *Optical Engineering* ,vol21, pp:427–31, 1982.
- [2] Sutton MA, Wolters WJ, Peters WH, Ranson WF, McNeill SR. “Determination of displacements using an improved digital image correlation method”. *Image and Vision Computing*, vol1,pp133–9, 1983.
- [3] Chu TC, Peters WH, Sutton MA, McNeil SR. “Application of digital image correlation to experimental mechanics’. *Image and Vision Computing*”. vol25, pp 232–45,1985.
- [4] Sutton MA, et al. “ Application of an optimized digital correlation method to planar deformation analysis”. *Image and Vision Computing*, vol4,pp143–50, 1986.
- [5] Sutton MA, Peters WH.et al. “Digital image correlation using Newton Raphson method of partial differential correction”. *Experimental Mechanics*; vol29, pp261–67, 1989.
- [6] Sutton MA, et al.. “Effects of subpixel image restoration on digital correlation error estimates”. *Optical Engineering*;vol27, pp 870–77, 1988
- [7] Wattrisse B, Chrysochoose A, Muracciole JM, Nemoz-Gaillard M. “Analysis of strain localization during tensile tests by digital image correlation”. *Experimental Mechanics*;vol41 ,pp29–39, 2001
- [8] Lu H, Cary PD. “Deformation measurements by digital image correlation: implementation of a second-order displacement gradient”. *Experimental Mechanics* ;vol40, pp 393–400, 2000
- [9] Jin GC, Wu Z, Bao N, Yao X. “Digital speckle correlation method with compensation technique for strain field measurements”. *Optical Laser Engineering* ;vol39,pp457–64,2003
- [10] Meng LB, Jin GC, Yao XF. “Application of iteration and finite element smoothing technique for displacement and strain measurement of digital speckle correlation”. *Optical Laser Engineering* ; vol45,pp57–63, 2007
- [11] Luo PF, Chao YJ, Sutton MA, Peters WH. “Accurate measurement of three-dimensional deformations in deformable and rigid bodies using computer vision”. *Experimental Mechanics*;vol33,pp 123–32, 1993.
- [12] McNeill SR, Sutton MA, Miao Z, Ma J. Measurement of surfaceprofile using digital image correlation. *Experimental Mechanics*;vol37, pp13–20,1997.

- [13] Wang Y, Cuitino AM.; “Full-field measurements of heterogeneous deformation patterns on polymeric foams using digital image correlation”. *International Journal of Solids Structure*;vol39,pp3777–96, 2002.
- [14] Meng LB, Jin GC, Yao XF, Yeh HY. ; “3D full-field deformation monitoring of fiber composite pressure vessel using 3D digital speckle correlation method”. *Polymer Testing journal* ;vol25,pp 42–8,2006
- [15] Han G, SuttonMA, Chao YJ.; “ Study of stationary crack-tip deformation fields in thin sheets by computer vision”. *Experimental Mechanics* ;vol34,pp 125–40,1994.
- [16] *MohammadrezaYadegariDehnav et.al*; “Utilizing digital image correlation to determine stress intensity factors,polymer testing” ,vol37,2009.
- [17] *Y.G. Wangan et.al.*; “A high resolution DIC technique for measuring small thermal expansion of film specimens” *Experimental Mechanics* ;vol25,pp 125–40,1994.
- [18] *Jay D. Carroll ,WaelAbuzaid , John Lambros , HuseyinSehitoglu.*; “High resolution digital image correlation measurements of strain accumulation in fatigue crack growth” *international journal of fatigue*,vol57,pp140-50,2010.
- [19] *Po-Chih Hung; A. S. Voloshin .et.al*; In-plane strain measurement by digital image Correlation, *journal of Brazilian society of mechanical sciences*,vol25, pp 215-21,2003.
- [20] *S. Tamulevicius, L. Augulis et.al* ; thermal strain measurements in graphite using electronic speckle pattern interferometry ,*vacuum* ,vol51, pp127,1998.
- [21] *C.J. Tay et.al.*;Digital image correlation for whole field out-of-plane displacement measurement using a single camera, *optics communications* ,vol.251 , pp 23-36,2005.
- [22] *Xiang Guo.et.al.*;Digital image correlation for large deformation applied in Ti alloy compression and tension test, *International journal for Light and electron optics*, vol. 125,pp 5316-5322,2014.
- [23] *Shun-Fa Hwang, Jhih-Te Horn, Hou-Jiun Wang*; Strain measurement of SU-8 photo resist by a digital image correlation method with a hybrid genetic algorithm, *Optics and lasers in engineering* ,vol.46, pp281-289,2008.
- [24] *M.A. Sutton .et.al*; “The effect of out-of-plane motion on 2D and 3D digital image correlation measurements”, *Optics and laser engineering* ,vol.46, pp746-57,2008.
- [25] *Zhengzong Tanga,et.al.* “Large deformation measurement scheme for 3D digital image correlation method”, *Optics and laser engineering* ,vol.50, pp122-130,2012.
- [26] *Rui Zhang , Lingfeng He.et.al* “Measurement of mixed-mode stress intensity factors using digital image correlation method”, *Optics and laser engineering*, vol.50,pp1001-07, 2012.

- [27] *Mohammad Kashfuddoja , R.G.R. Prasath , M. Ramjia*; “Study on experimental characterization of carbon fiber reinforced polymer panel using digital image correlation.” *Optics and laser engineering*, Vol.62,pp17-30,2008.
- [28] *Xiangjun Dai , Fujun Yang , Zhenning Chen , Xinxing Shao , Xiaoyuan He*; “Strain field estimation based on digital image correlation and radial basis function,” *Optics and laser engineering* ,vol.65,pp64-72, 2015.
- [29] *Yue Gao, Teng Cheng n, Yong Su, Xiaohai Xu, Yong Zhang, Qingchuan Zhang*; “High-efficiency and high-accuracy digital image correlation for three-dimensional measurement”, *Optics and laser engineering* ,vol.65,pp73-80,2015
- [30] *K.M. Saranath et al.* “Zone wise local characterization of welds using digital image correlation technique” *Optics and laser engineering* ,vol63,pp30-42, 2014.
- [31] *Jinlong Chen, Nan Zhan , Xiaochuan Zhang , Jixiao Wang*; “Improved extended digital image correlation for crack tip deformation measurement”, *Optics and laser engineering* ,.vol.63,pp 60-72,2014
- [32] *Zhenyu Jiang.et al.*; “Path-independent digital image correlation with high accuracy, speed and robustness”. *Optics and laser engineering*, vol.65, pp 93-102, 2015.
- [33] *FeipengZhu et al.*; “Measurement of true stress–strain curves and evolution of plasticzone of low carbon steel under uniaxial tension using digital image correlation”. *Optics and laser engineering*,vol.62,pp103-110,2014.
- [34] *T.L.Jin. et al.*; “A study of the thermal buckling behavior of a circular aluminum plate using the digital image correlation technique and finite element analysis”. *Thin walled structure*,vol.77,pp187-197,2014.
- [35] *François Hild .et al.*; “Calibration of constitutive models of steel beams subject to local buckling by using digital image correlation”. *Chemometrics and Intelligent Labrotary Systems*,vol.120,pp15-24,2012.
- [36] *Fabienne Lagattu. et al.*; “High strain gradient measurements by using digital image correlation technique”. *Material chrecterization*,Vol.53,pp17-28,2004.
- [37] *Fabienne Lagattu.et.al.*; “In-plane strain measurements on a microscopic scale by coupling digital image correlation and an in situ SEM technique”. *Material chrecterization*,Vol.56,pp10-18,2006.
- [38] *M. Koster.ET.AL.*; “Digital image correlation for the characterization of fatigue damage evolution in brazed steel joints”. *Procedia Materials science*, Vol.3,pp1117-122, 2014.
- [39] *Introducing Solidworks 2013 manual from Dassault corporation 2013.*